DEPARTAMENTO DE CIÊNCIAS DA VIDA

FACULDADE DE CIÊNCIAS E TECNOLOGIA
UNIVERSIDADE DE COIMBRA

Mitochondria in glutamatergic nerve terminals are selectively affected by exposure to $A\beta_{1-42}$ modeling early Alzheimer's disease

Dissertação apresentada à Universidade de Coimbra para cumprimento dos requisitos necessários à obtenção do grau de Mestre em Biologia Celular e Molecular, realizada sob a orientação científica do Professor Doutor Carlos Palmeira (Universidade de Coimbra) e do Professor Doutor Rodrigo Cunha (Universidade de Coimbra)

João Filipe Alves Amorim

2014

Este trabalho foi realizado no Centro de Neurociências e Biologia Celular, em Coimbra, no Grupo "Neuromodulation" ("Purines at CNC")

Agradecimentos/Acknowledgments

Ao meu orientador, o Professor Carlos Palmeira, o meu muito obrigado por toda a disponibilidade e apoio demonstrado ao longo deste ano, tornando-se para mim um suporte fundamental ao longo destes últimos meses. Por ter contribuído para a minha formação cientifica, mas acima de tudo pela amizade, simpatia e concelhos demonstrados o meu obrigado!

Ao meu coorientador, o Professor Rodrigo Cunha, o meu muito obrigado por toda a disponibilidade e apoio demonstrados. Pela oportunidade de trabalhar no seu laboratório e por toda a sabedoria transmitida ao longo deste ultimo ano o meu obrigado!

À Paula Canas o meu muito obrigado pela incansável disponibilidade demonstrada, por todo o conhecimento transmitido assim como pela rigorosa partilha de conhecimentos que em muito contribuiu para enriquecer esta ainda curta carreira científica.

À Professora Anabela Rolo, o meu muito obrigado por toda a disponibilidade e apoio demonstrado assim como pelos conselhos sábios transmitidos ao longo deste ultimo ano.

Ao Professor Ângelo Tomé e ao Ricardo Rodrigues o meu muito obrigado por todos os conhecimentos transmitidos, sempre com discussões muito enriquecedoras, que muito contribuíram para a elaboração deste trabalho, assim como pela disponibilidade sempre demonstrada.

Aos meus colegas de grupo, Anna Pliássova e Filipe Duarte, o meu muito obrigado por toda a ajuda e disponibilidade prestada ao longo deste ano.

À Renata, o meu muito obrigado pela incansável paciência demonstrada, assim como por todo o apoio, amizade e carinho transmitidos, dando-me força nos momentos mais difíceis.

Aos meus pais e irmã o meu muito obrigado por todo o apoio, motivação, carinho e coragem demonstrados, que sempre tudo fizeram para que pudesse ultrapassar mais uma etapa na minha vida.

A todos os meus colegas de grupos e a todos os amigos que me acompanharam durante este ano o meu muito obrigado pela amizade e por todos os momentos partilhados.

A todo o pessoal do CNC que de algum modo me ajudaram ao longe deste ano, o meu obrigado!

Contents

List of figures

List of tables

Abbreviations

$^{\cdot}O_2^-$	Free radical superoxide
$[Ca^{2+}]_c$	Cytosolic calcium
$[Ca^{2+}]_m$	Intra-mitochondrial calcium
$\Delta\mu_{H+}$	Electrochemical gradient
Δp	Proton motive force
ΔpH	H^+ gradient across the inner membrane
$\Delta\psi_m$	Mitochondrial membrane potential
$\Delta\psi_p$	Plasma membrane potential
ABAD	Aβ-binding alcohol dehydrogenase
AD	Alzheimer's disease
ADP	Adenosine 5'-diphosphate
AICD	Intracellular carboxyl-terminal domain of APP
AIF	Apoptosis-inducing factor
ANT	Adenine nucleotide translocator
APP	Amyloid precursor protein
ATP	Adenosine 5'-triphosphate
AZ	Active zone
Aβ	Amyloid-β peptide
BAK	BCL-2 antagonist/killer
BAX	BCL-2-associated X protein
BCL-2	Pro-apoptotic B-cell lymphoma protein 2
BID	BH3-interacting domain death agonist
BSA	Bovine serum albumin
CCCP	Carbonyl cyanide chlorophenyl hydrazine
CNS	Central nervous system
Complex I	NADH-ubiquinone oxidoreductase
Complex II	Succinate-ubiquinone oxidoreductase
Complex III	Ubiquinol-cytochrome oxidoreductase
Complex IV	Cytochrome c oxidase
Complex V	ATP synthase or F_0F_1 ATPase
CSK	Cytoskeleton
CTF	Carboxyl-terminal fragment of APP
CypD	Cyclophilin D
Cyt c	Cytochrome c
DIABLO	Direct IAP-binding protein with low PI
DiOC6	3,3'-dihexyloxacarbocyanine iodide
DMSO	Dimethylsulfoxide
DNA	Deoxyribonucleic acid
Drp-1	Dynamin-like protein-1
DTT	Dithiothreitol
EDTA	Ethylenediaminetetraacetic acid
ER	Endoplasmic reticulum
ETC	Electron transport chain
EtOH	Ethanol
$FADH_2$	Flavin adenine dinucleotide (hydroquinone form)
FCCP	Cyanide *p*-(trifluoromethoxy)phenylhydrazone

GPX	Glutathione peroxidase
GR	Glutamate receptor
GSH	Glutathione
GTP	Guanosine 5'-triphosphate
H_2O	Water
H_2O_2	Hydrogen peroxide
HBM	Hepes buffered medium
HEPES	2-[4-(2-hydroxyethyl)piperazin-1-yl]ethanesulfonic acid
hFis1	Outer mitochondrial membrane protein 1
IAP	Inhibitor of apoptosis protein
JC-1	5,5',6,6'-tetrachloro-1,1',3,3'-tetraethylbenzimidazolylcarbocyanine iodide
KC	Kinase cascade
KCl	Potassium chloride
Krebs cycle	Tricarboxylic acid cycle
LETM1	Leucine-zipper EF-hand-containing transmembrane protein 1
MCU	Mitochondrial calcium uniporter
Mff	Mitochondrial fission factor
Mfn	Mitofusins
MICU1	Mitochondrial calcium-uptake 1
Mn-SOD	Manganese superoxide dismutase
mPTP	Mitochondrial permeability transition pore
MT	Microtubules
MT	Microtubule
mtDNA	Mitochondrial DNA
mtTFA	Mitochondrial transcription factor A
NAD^+	Nicotinamide adenine dinucleotide (oxidized form)
NADH	Nicotinamide adenine dinucleotide (reduced form)
NADPH	Nicotinamide adenine dinucleotide phosphate
NCLX	Na^+/Ca^{2+} exchanger
NFTs	Neurofibrillary tangles
NHS	Normal horse serum
NMJ	Neuromuscular junctions
NO	Nitric oxide
NOS	Nitric oxide synthase
NRF	Nuclear respiratory factor
NTF	Neurotrophic factor
O_2	Oxygen
OPA1	Optic atrophy protein 1
Par-4	Prostate apoptosis response 4
PBS	Phosphate buffered saline
PCD	Programmed cell death
PGC 1α	Peroxisome proliferator-activated receptor gamma coactivator-1α
Pi	Phosphate
PMPI	Plasma membrane potential indicator
PO_4^{3-}	Phosphate ion
PRX	Peroxiredoxin
PS-1/2	Presenilin-1/2
PSD-95	Postsynaptic density protein 95

Rod 123	Rhodamine 123
ROS	Reactive oxygen species
RT	Room temperature
SEM	Standard Error of the Mean
SLP2	Stomatin-like protein 2
tBID	BH3-interacting domain death agonist (truncated form)
TF	Transcription factor
TIM	Mitochondrial inner membrane protein insertion complex
TMRE	tetramethylrhodamine ethyl ester
TMRM	Tetramethylrhodamine methyl ester
TOM	Mitochondrial outer membrane multisubunit protein complex
TPP^+	Tetraphenylphosphonium
TRX	Thioredoxin
VDAC	Voltage-dependent anion channel
VDCC	Voltage-dependent calcium channel
VGLUT1	Vesicular glutamate transporter 1
VGLUT2	Vesicular glutamate transporter 2
VGLUT3	Vesicular glutamate transporter 3
VGLUTs	Vesicular glutamate transporters

ABSTRACT

Alzheimer's disease (AD) is defined by a loss of cognitive function associated with an abnormal processing and accumulation of amyloid β-peptide (namely $A\beta_{1-42}$) and by a hypometabolism and hypofunction of brain cortical regions, mainly the hippocampus. With the aim to arrest the evolution of AD, particular attention has been devoted to synaptic dysfunction and loss, which are one of the precocious modifications accompanying cognitive dysfunction. Mitochondria play a key role in the maintenance of adequate synaptic function and mitochondrial structural and functional abnormalities are well characterized features of AD. Additionally, mitochondrial accumulation of amyloid β-peptide (Aβ) was shown to occur before extracellular Aβ deposition. On the other hand, a predominant susceptibility of glutamatergic synapses was already described, using an Aβ-based model of AD. This prompted us to post the hypothesis that mitochondria located in glutamatergic terminals are particularly affected in AD, leading to modifications of calcium dynamics and energy supply that underlie the synaptic degeneration in AD.

The main goals of this work were to: i) optimize a protocol to measure *in situ* the mitochondrial membrane potential Δ ($\Delta\psi_m$) in single nerve terminals and ii) assess if presynaptic mitochondria located in glutamatergic nerve terminals are particularly affected in an *in vitro* model of AD. Hippocampal nerve terminals, obtained through a discontinuous Percoll gradient, were incubated with oligomeric $A\beta_{1-42}$ peptide to analyze through live imaging experiments the changes of $\Delta\psi_m$.

We observed a reduction of $\Delta\psi_m$ in the total population of hippocampal nerve terminals after incubation with 500 nM of the $A\beta_{1-42}$ peptide, without any modification in plasma membrane potential ($\Delta\psi_p$). Notably, we observed that $A\beta_{1-42}$ caused a selective decrease of $\Delta\psi_m$ in glutamatergic terminals whereas it did not affect $\Delta\psi_m$ in non-glutamatergic terminals.

These results are in agreement with the contention that synaptic mitochondria are an important trigger of "synaptic apoptosis", contributing to synaptic dysfunction and degeneration in AD and further indicate glutamatergic terminals as primary targets of $A\beta_{1-}$

$_{42}$-induced toxicity. This prompts the correction of synaptic mitochondria dysfunction as a justifiable candidate to therapeutically alleviate early AD.

Keywords: Alzheimer's disease, amyloid β-peptide, synaptic mitochondria, mitochondrial membrane potential, synaptic loss.

RESUMO

A doença de Alzheimer (DA) é definida pela perda de função cognitiva associada ao processamento anormal e acumulação do peptídeo β-amilóide (nomeadamente $A\beta_{1-42}$) assim como pelo hipometabolismo e hipofunção de regiões corticais do cérebro, principalmente no hipocampo. Com o objetivo de deter a evolução da DA, tem sido dedicada particular atenção à disfunção e perda sinápticas, dado que estas são modificações precoces que acompanham a disfunção cognitiva. As mitocôndrias desempenham um papel fundamental na manutenção da função sináptica adequada, com anormalidades estruturais e funcionais nas mitocondriais sendo bem descritas na DA. Além disso, foi demonstrado que a acumulação mitocondrial de Aβ precede a deposição extracelular. Por outro lado, num modelo de DA baseado na administração de Aβ, foi descrita a predominante susceptibilidade das sinapses glutamatérgicas. Estas evidências levaram-nos a colocar a hipótese de que as mitocôndrias localizadas em terminais glutamatérgicos são particularmente afetadas na DA, perturbando a homeostase do cálcio assim como a disponibilidade energética, fatores que estão na base da degeneração sináptica na DA.

Os principais objetivos deste trabalho foram: i) a otimização de um protocolo para avaliar *in situ* o potencial de membrana mitocondrial Δ ($\Delta\psi_m$) em terminais nervosos individuais e ii) avaliar se as mitocôndrias pré-sinápticas localizadas nos terminais nervosos glutamatérgicos são particularmente afetadas num modelo *in vitro* da DA. Terminais nervosos do hipocampo obtidos através de um gradiente descontínuo de Percoll foram incubados com o peptídeo $A\beta_{1-42}$ na sua forma oligomérica e análises qualitativas através de experiências de "live imaging" foram feitas com o objetivo de avaliar as diferenças do $\Delta\psi_m$.

Observou-se uma redução no $\Delta\psi_m$, sobretudo nos terminais nervosos glutamatérgicos, após incubação com o peptídeo $A\beta_{1-42}$, sem qualquer modificação no potencial de membrana plasmática ($\Delta\psi_p$).

Estes resultados suportam o papel das mitocôndrias sinápticas como um importante gatilho de "apoptose sináptica", contribuindo para a disfunção e degeneração sináptica na DA. Indicam ainda os terminais glutamatérgicos como principais alvos da toxicidade induzida pelo peptídeo $A\beta_{1-42}$. Assim, a correção da disfunção de mitocôndrias sinápticas é cada vez mais um candidato justificável para aliviar terapeuticamente estados precoces da DA.

Palavras-chave: Doença de Alzheimer, péptido β-amilóide, mitocôndria sináptica, potencial de membrana mitocondrial, perda sináptica.

1.INTRODUCTION

The human brain has one of the most striking features in the human body. Despite the fact that it occupies less than 2% of the body mass, it consumes 20% of total resting metabolic energy (Moreira *et al.* 2010). Most of this energy is consumed by neurons, highly specialized cells facing unique challenges in carrying out their important physiological functions mainly on reversing the ion fluxes underlying action potential generation and synaptic transmission (Attwell & Laughlin 2001). Mitochondrial function is crucial for neurons to face their challenges. Since glycolytic capacity of neurons is limited, neurons are almost entirely dependent on aerobic oxidative phosphorylation through mitochondria (Zhu *et al.* 2013), which are highly efficient organelles in utilizing oxygen (O_2) and substrates, mostly derived from glucose to generate cellular energy in form of adenosine triphosphate (ATP) (Macaskill & Kittler 2009). Besides the dependence on ATP production, important for many processes and ATP-dependent identities such as ion channels, pumps, receptors, vesicles and recycling neurotransmitters (Chan 2006; Hoppins *et al.* 2007; Zhang & Chan 2007), neurons are also dependent on mitochondria for maintenance of calcium (Ca^{2+}) homeostasis either the clearance of calcium by direct calcium removal or by providing ATP for plasma membrane Ca^{2+}-ATPase and Na^{+}/Ca^{2+} exchanger (Su *et al.* 2010). Thus, it is logical to consider that mitochondria must be located close to these sites where synaptic and action potentials are generated by ion influxes (Macaskill & Kittler 2009).

In Alzheimer's disease (AD), as well as in all neurological disorders associated with mitochondria abnormalities, the fundamental pathophysiological mechanisms remain unclear. Understanding the extent of these changes in mitochondrial function and elucidating if these changes represent primary or secondary components of the pathophysiological process, as well as understanding the basic pathways that lead to the development of disease, represent major challenges of the contemporary neurosciences.

1.1. Mitochondria in the Brain

Mitochondria, first described 100 years ago (Lewis & Lewis 1914), form a highly complex organellar network in eukaryotic cells, either in terms of distribution or morphology. These organelles can be found at various intracellular locations with high energy demand, such as, pre- and post-synaptic domains, the axon initial segments, nodes of Ranvier and growth cones (Hollenbeck & Saxton 2005).

1.1.1. Mitochondria Physiology and Bioenergetics

Considered as the "biochemical powerhouse" of the cell, mitochondria are dynamic and plastic organelles composed by two different membranes - inner mitochondrial membrane and outer mitochondrial membrane, an intermembranar space and a matrix. Within and across the inner one, a molecular machinery associated with electron flow, the electron transport chain (ETC), is organized and in an assembly-like manner. This chain combines the sequential activity of five protein complexes, namely complex I (NADH-ubiquinone oxidoreductase), II (succinate-ubiquinone oxidoreductase), III (ubiquinol-cytochrome oxidoreductase), and IV (cytochrome c oxidase). Complex I and II receive, respectively, electrons from nicotinamide adenine dinucleotide (NADH) and flavin adenine dinucleotide ($FADH_2$) and electrons are transferred through oxidoreduction reactions to Complex III (via ubiquinone or coenzyme Q_{10}) and then to Complex IV (via cytochrome c – Cyt c) (Mattson *et al.* 2008) where O_2 is consumed as final electron acceptor. In parallel, a proton (H^+) efflux is driven toward the intermembranar space via H^+ pumps in complex I, III and IV generating an electrochemical gradient ($\Delta\mu_{H+}$) the proton motive force (Δp). At 37 ^oC, $\Delta p = \Delta\psi_m - 60\Delta pH$ (where $\Delta\psi_m$ corresponds to the mitochondrial membrane potential, and ΔpH corresponds to the H^+ gradient across the inner membrane). $\Delta\psi_m$ (the dominant component of Δp) and Δp are often interchangeably referred to the common driven force for key mitochondrial functions (Nicholls & Budd 2000); however, while Δp correspond to the primary bioenergetic parameter controlling mitochondrial ATP synthesis, $\Delta\psi_m$ regulates mitochondrial Ca^{2+} uptake and reactive oxygen species (ROS)

generation (Nicholls & Ward 2000). $\Delta\psi_m$ is therefore considered a central parameter of mitochondrial function (Duchen 2000; Ward *et al.* 2000).

ATP production arises from glucose and O_2 through a cascade of processes beginning with glycolysis and ending on oxidative phosphorylation (glycolysis -> pyruvate decarboxylation -> tricarboxylic acid cycle -> oxidative phosphorylation). Almost all these processes occur within mitochondria, while only glycolysis takes place in the cytosol. The movement of H^+ ions back into the matrix is driven by ATP synthase (Complex V or F_0F_1 ATPase) (Duchen 2004) and allows the production of ATP from adenosine diphosphate (ADP) and phosphate (Pi) closing the proton circuit established by respiratory chain activity. ATP is then exported to the cytosol via the adenine nucleotide translocase (ANT) by exchange with ADP (Figure 1). The inward transport of ATP favors a net inward positive charge and consequently tends again to a slight depolarization of the mitochondrial potential when compared to the cytosol (Duchen 2004). This potential is estimated between -150 mV and -180 mV (Macaskill & Kittler 2009). Importantly, the ATP synthase activity may be reversed by mitochondria consuming rather than producing ATP. Transient ATP synthase reversal may in fact support Δp maintenance, crucial for mitochondrial activity; however unrestricted reversal may lead to cellular ATP depletion (Campanella *et al.* 2009).

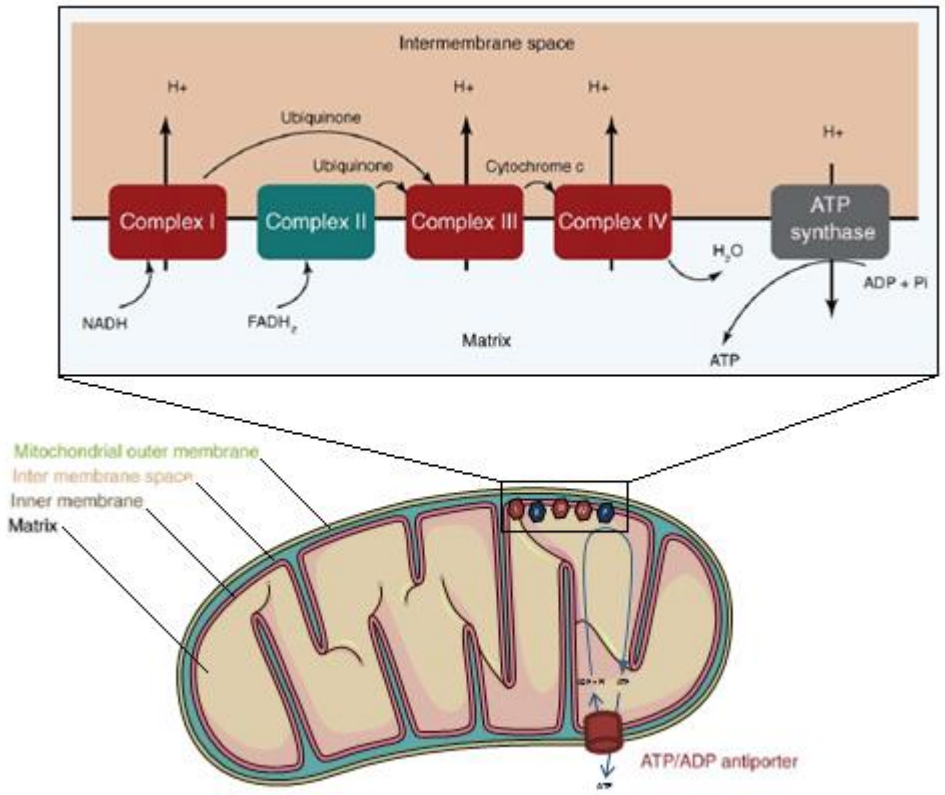

Figure 1: The oxidative phosphorylation chain (adapted from (Macaskill & Kittler 2009)). Glycolysis and the tricarboxylic acid cycle (Krebs cycle), using carbon substrates produce NADH, which enters the chain at complex I, and $FADH_2$, which enters the chain at complex II. Ubiquitin is responsible for the transfer of electrons from both complex I and complex II to complex III and then Cyt c is responsible for the transfer of electrons to complex IV. In the complex IV, the electrons are used to produce water (H_2O) from O_2 (final electron acceptor). The flow of electrons generates energy, which in turn is used by complexes I, III and IV to translocate H^+ across the membrane creating a proton motive force. Finally, the dissipation of this proton gradient is used by the ATP synthase as well as other mitochondrial processes, such Ca^{2+} buffering.

1.1.2. Mitochondrial Calcium Handling

The role of mitochondrial in Ca^{2+} homeostasis (Jonas 2006; MacAskill *et al.* 2010; Gleichmann & Mattson 2011) is fundamental for cell metabolism, proliferation, differentiation and death (Patergnani *et al.* 2011). Mitochondria are modulators of cytosolic Ca^{2+} concentration ($[Ca^{2+}]_c$) displaying a high capacity for Ca^{2+} storage. This is particularly important in neurons, which are excitable cells with frequent sudden and extensive $[Ca^{2+}]_c$ increases, where mitochondria prevents cytosolic Ca^{2+} overload by Ca^{2+} sequestration (Kann & Kova 2007).

Mitochondrial Ca^{2+} uptake, or Ca^{2+} influx to the mitochondrial matrix, is primarily driven by the electrochemical potential gradient established by the $\Delta\psi_m$ and is increased in situations of high cytosolic Ca^{2+} concentrations and in situations of high energy demand (Duchen 2004), when the ATP/ADP ratio is low. On the other hand, this influx decreases in situations of low cytosolic Ca^{2+} levels and high ATP/ADP ratios. The negative membrane potential drives Ca^{2+} influx which in turn occurs over at least two mechanisms: mitochondrial calcium uniporter (MCU) and leucine-zipper EF-hand-containing transmembrane protein 1 (LETM1) (Patergnani *et al.* 2011) (Figure 2). As consequence of these high levels of Ca^{2+} within mitochondrial matrix, the activity of three Krebs cycle enzymes (pyruvate dehydrogenase, isocitrate dehydrogenase and α-ketoglutarate dehydrogenase) and ATP synthase also increase, bolstering ATP production (Gleichmann & Mattson 2011). Ca^{2+} can also be buffered (most likely by converting it to an insoluble $(Ca)_x(PO_4)_y(OH)_z$ salt due to the reaction of Ca^{2+} with PO_4^{3-} provided by a Pi carrier) or it can be transported again back to cytosol via a Na^+/Ca^{2+} antiporter powered by a sodium gradient set up by a Na^+/H^+ antiporter (Szabadkai & Duchen 2008) (Figure 2). At least two mechanisms have been described regarding the efflux of matrix Ca^{2+} toward cytosol: the Na^+/Ca^{2+} exchanger (NCLX) and the mitochondrial permeability transition pore (mPTP) (Jonas 2006; Patergnani *et al.* 2011) (Figure 2). ATP produced during oxidative phosphorylation is also used as fuel to pump out the intracellular Ca^{2+} by mitochondria (Gleichmann & Mattson 2011).

In addition to the well characterized role of inner mitochondrial membrane in the control of cytosolic or mitochondrial Ca^{2+} concentration, the role of the outer mitochondrial membrane has not been directly accessed. The outer mitochondrial membrane is permeant to small ions but it may have a secondary role in modulating the access of Ca^{2+} to the uniporter, through the voltage-dependent anion channel (VDAC). This is a selectively filter that may be associated with the outer mitochondrial membrane Ca^{2+} permeability (Gincel *et al.* 2001). Additionally, it has also been suggested that VDAC appears to be part of the mPTP, a pore which is regulated by intramitochondrial Ca^{2+} concentration ($[Ca^{2+}]_m$) (Duchen 2004).

Still, mitochondrial has a limited Ca^{2+} buffering capacity, and it is becoming clear that elevation of free $[Ca^{2+}]_c$ is critical for many types of neuronal cell death (Choi 1992). Nicholls and Budd (2000) estimated that, in the presence of physiological amounts of Pi, mitochondria can accumulate and retain mM concentrations of Ca^{2+} (Nicholls & Budd 2000). Nevertheless, deleterious effects arise due excessive accumulation of Ca^{2+} leading to the opening of the mPTP and to the deposition of Ca^{2+}-phosphate precipitates. However, the phosphate complexes are reversible, and when plasmalemmal Ca^{2+} pumps reestablish $[Ca^{2+}]_c$ below the set point, Ca^{2+} is gradually released in the cytosol by mitochondria (Nicholls & Chalmers 2004).

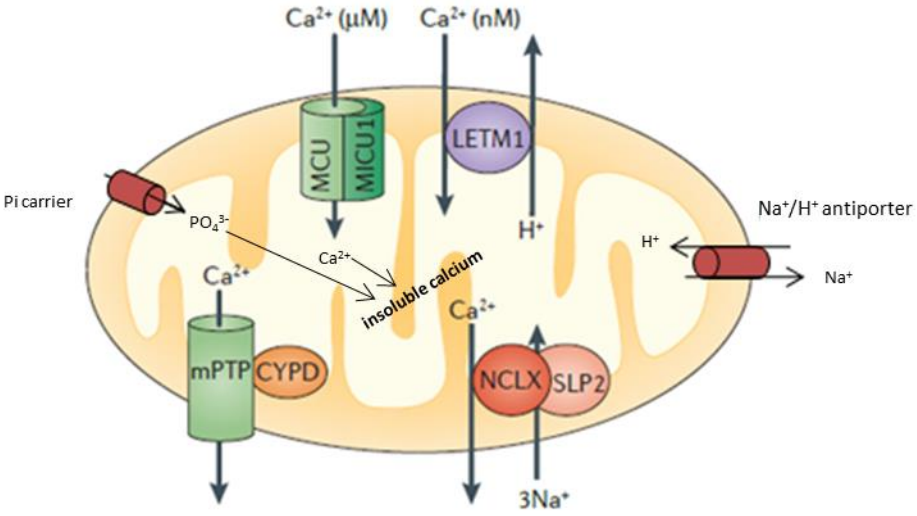

Figure 2: **Calcium regulation by mitochondria (adapted from (Manji *et al.* 2012)).** The outer mitochondrial membrane, unlike the inner mitochondrial membrane, is permeable to Ca^{2+} allowing its influx toward mitochondrial matrix. Driven by the negative membrane potential, Ca^{2+} influx occurs through two types of importers: MCU, which as low calcium affinity operating in the micromolar range of cytosolic Ca^{2+} concentrations, and LETM1. Mitochondrial calcium-uptake (MICU1), a calcium sensor, is responsible for regulation of the Ca^{2+}-influx capacity of MCU. The import of cytosolic Ca^{2+} in the nanomolar range is allowed by LETM1, a high-affinity mitochondrial Ca^{2+}/H^{+} exchanger. The efflux of Ca^{2+}, on the other hand, occurs through a NCLX exchanger, which can also mediate Li^{+}/Ca^{2+} exchange. Stomatin-like protein 2 (SLP2), which is located at the inner mitochondrial membrane, negatively regulate NCLX activity. At high matrix Ca^{2+} levels, the protein complex mPTP opens. Cyclophilin D (CypD) has a role in the opening of mPTP by desensitizing the mPTP to Ca^{2+} and thus facilitates the permeability transition pore opening.

1.1.3. Reactive Oxygen Species

Mitochondria use at least 90% of the O_2 available in the cells to produce ATP, and therefore mitochondria becomes the major intracellular producer of ROS (Mattson *et al.* 2008; Massaad & Klann 2011) causing a tremendous endogenous oxidative burden. These highly reactive free radicals can induce oxidative damage to carbohydrates, lipids (through lipid peroxidation), proteins (through conversion of phenylalanine to m-tyrosine and o-tyrosine) and DNA (through mutagenesis) (Manji *et al.* 2012) including mitochondrial DNA

(mtDNA), which has no association with histones and consequently is less protected from radical damage than nuclear DNA (Duchen 2004).

Superoxide ($^{\cdot}O_2^-$) is produced at the ETC due incomplete reduction of O_2 during oxidative phosphorylation. Thus, in the presence of substrates and in the absence of ADP, the ETC becomes highly reduced, increasing the likelihood of electrons "slipping" from ETC to O_2, reducing O_2 with one electron to $^{\cdot}O_2^-$ (Turrens 2003; Balaban *et al.* 2005; Murphy 2009). However, mitochondrial defense mechanisms are available. $^{\cdot}O_2^-$ is efficiently dismutated to hydrogen peroxide (H_2O_2) by Mn^{2+}-dependent superoxide dismutase (Mn-SOD) and subsequently transformed to H_2O by glutathione peroxidase (GPX) and peroxiredoxin (PRX). This late reaction depends on the regeneration of the reduced species of both glutathione (GSH) and thioredoxin (TRX) (Ying 2008; Aon *et al.* 2012). Accordingly, the Krebs cycle has a central role in the quenching of oxygen radical species, in addition to the provision of electron carriers (NADH and $FADH_2$) for ATP production at the ETC. The production of nicotinamide adenine dinucleotide phosphate (NADPH) through enzymes that depend on Krebs cycle subtracts (Ying 2008), is then used to reduce the redox states of GSH and TRX regenerating the antioxidant capacity of the mitochondrial matrix (Garcia *et al.* 2010; Nickel *et al.* 2014).

Mitochondrial ROS production thus, has been related with NADH/NAD^+ redox state and $\Delta\psi_m$ (Starkov & Fiskum 2003). Keelan and colleagues (Keelan *et al.* 1999) found that nitric oxide (NO) exposure in combination with an otherwise innocuous Ca^{2+} load caused mitochondrial depolarization leading them to suggest that elevation $[Ca^{2+}]_c$ acts synergistically with NO to amplify mitochondrial depolarization and impairing $[Ca^{2+}]_c$ homeostasis. Additionally, Dmitry Zorov and colleagues (Zorov *et al.* 2006) postulated that ROS, above a certain level, could trigger mitochondrial membrane depolarization. Hence, Chontida Yarana and colleagues (Yarana *et al.* 2012) suggested that increases in Ca^{2+} threshold levels might induce an increase of the ROS to levels high enough to cause $\Delta\psi_m$ dissipation.

1.1.4. Neuronal Cell Death

1.1.4.1. Programmed Cell Death

In addition to contributing to cell survival, mitochondria have also an important role in cell death. Apoptosis is a prototypal form of programmed cell death (PCD) in neurons, which may occur in diverse neurodegenerative conditions. Morphologically, apoptosis can be characterized by cell shrinkage, membrane blebbing and karyorhexis (nuclear fragmentation) (Mattson *et al.* 2008). Apoptosis, a genetically predetermined mechanism, may be prompted by several mechanisms being the extrinsic pathway, activated by ligation of death receptors, and the intrinsic pathway, emerging from mitochondria, the most prominent and best characterized pathways. Mitochondria play a role in both pathways leading to apoptosis (Manji *et al.* 2012).

The extrinsic pathway, also known as death receptor pathway, requires the activation of death receptors such as tumor necrosis factor-α receptor 1 and Fas receptor, also called CD95/Fas or Apo-1/Fas receptor (Strasser *et al.* 2009). The activation of these receptors on the cell surface triggers the activation of a cascade of cysteine-protease enzymes, which are present in synapses and dendrites of neurons and where they can be activated in response to Ca^{2+} influx, through protein-protein interactions leading to apoptosis (Shoshan-Barmatz & Ben-Hail 2012). In the extrinsic pathway, caspase-8 and possibly caspase-10 are activated, leading to consequent activation of effector caspases-3, -6 and -7 (Kroemer *et al.* 2007). Activated caspases-8 cleave BH3-interacting domain death agonist (BID) to its truncated form (tBID) facilitating its translocation to mitochondria, where its action is similar to other pro-apoptotic B-cell lymphoma protein 2 (BCL-2) family members, such as BCL-2-associated X protein (BAX) and BCL-2 antagonist/killer (BAK) proteins. These proteins alter membrane permeability, leading to leakage of apoptogenic factors, and, consequently, apoptosis (Shoshan-Barmatz & Ben-Hail 2012).

The intrinsic pathway predominates in neurons (Mattson *et al.* 2008) and is activated by several cell death signals, such as high levels of cytoplasmic Ca^{2+} and ROS, damage caused by ultraviolet radiation, DNA damage and increased expression of the proapoptotic BCL-2 family members (BAX and BAK) (Mattson *et al.* 2008; Manji *et al.* 2012). These

different stimuli trigger BAX and BAK to form pores in the outer mitochondrial membrane leading to increase in mitochondrial permeability of these membrane, without decreased inner membrane integrity, which consequently may release several killing molecules (Dong *et al.* 2006). Additionally, the outer mitochondrial membrane may also be involved in the formation of the mPTP. The mPTP, a scaffold structure based on dynamic interactions between VDAC in the outer membrane, ANT in the inner membrane and CypD (mitochondrial matrix protein) (Zoratti & Szabó 1994; Zoratti & Szabb 1995), build up contact sites between the outer and inner mitochondrial membrane. Increase in mitochondrial permeability transition will result in the formation of this pore, which leads to the flux of solutes and H_2O into mitochondria and, as result, swelling the matrix (Dong *et al.* 2006).

The mPTP causes a leak of Cyt c, apoptosis-inducing factor (AIF), DIABLO (also referred as second mitochondria-derived activator of caspases (SMAC)) and endonucleases (Youle & Strasser 2008; Shoshan-Barmatz & Ben-Hail 2012) from the mitochondrial intermembranous space into the cytosol. Once in cytosol, they activate caspases leading to apoptosis (Youle & Strasser 2008; Shoshan-Barmatz & Ben-Hail 2012).

In neurons, apoptosis occurs upon ischemia, brain traumatic injury and a variety of neurodegenerative conditions (Hunsberger *et al.* 2009). However, while apoptotic PCD encompasses the whole cell, apoptotic mitochondrial biochemical cascades can be triggered locally within synapses. Activation of mitochondrial apoptotic cascade could lead to “synaptic apoptosis” (Culmsee & Mattson 2005) affecting individual synapse. These hypotheses suggest a mechanism for synaptic loss in both physiological and pathological process (Mattson *et al.* 1998a; Mattson *et al.* 2008).

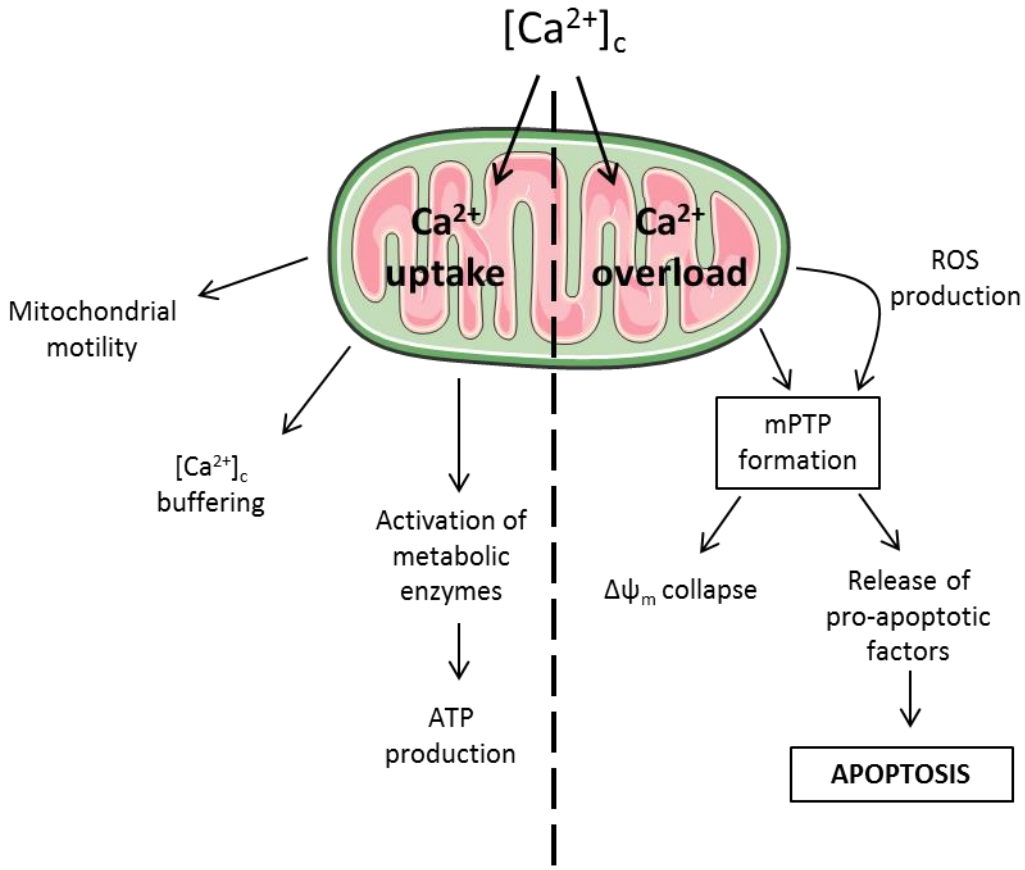

Figure 3: **Mitochondrial life and death pathways.** Extensive Ca^{2+} influx may result in Ca^{2+} overload which consequently exacerbate ROS formation, induction of mPTP, $\Delta\psi_m$ collapse and finally, apoptosis.

1.1.5. Mitochondrial Biogenesis and Dynamics

Mitochondria in neurons, as well as in many other cell types, have the particularity to be maintained as short tubular structures being highly dynamic, where they can move, divide and fuse (Frederick & Shaw 2007; Kageyama *et al.* 2011; Westermann 2012). During neuronal lifespan, mitochondria are continuously regenerated through biogenesis. On the other hand, damaged mitochondrial can be degraded by mitophagy (mitochondria autophagy) in order to prevent the release of apoptotic factors which can induce neuronal death.

Nevertheless, biogenesis, the increase in mitochondrial mass, requires the interplay between the nuclear and the mtDNA. Since the mitochondrial genome is insufficient for independent replication, ~1000 different nuclear-encoded proteins synthetized in the cytosol, are imported to the mitochondria in an unfolded state. This process is supported by the outer and inner membrane components of the TOM complex, the translocase Tom and Tim respectively (Mokranjac & Neupert 2008). Moreover, several transcription factors assist mitochondrial biogenesis, namely mitochondrial transcription factor A (mtTFA), nuclear respiratory factors (NRF-1 and NRF-2), and peroxisome proliferator-activated receptor gamma coactivator-1α (PGC-1α) (Medeiros 2008). As mentioned earlier, mitochondrial biogenesis is highly dependent on the transfer of nuclear-encoded preproteins across and into the mitochondrial membranes. However, while some of these steps can occur in absence of $\Delta\psi_m$ or ATP, such as some action on TOM complex, others, such as the import via the TIM-23 complex toward the matrix, require both $\Delta\psi_m$ and ATP in the matrix. Furthermore, $\Delta\psi_m$ but not ATP, is also required for the insertion of hydrophobic proteins into the inner membrane via TIM-22 (Bauer & Neupert 2001; Mokranjac & Neupert 2008). Also the establishment of mitochondrial $\Delta\psi_m$ appears essential for an effective preprotein import, and normal mitochondrial biogenesis. Thus, abnormal mitochondrial preprotein import, a $\Delta\psi_m$-dependent process, is a likely mechanism involved in the progression of neurodegeneration.

Mitochondrial fission and fusion are responsible for the establishment of organelle size, number and shape allowing the mixing of mitochondrial contents, such as proteins and lipids, including mtDNA (Itoh *et al.* 2013).

Mitochondrial fusion and fission are membrane-remodeling events assisted by enzyme machinery, involving several evolutionary conserved GTPases. Fusion of the outer membrane is promoted by mitofusins (Mfn 1 and Mfn 2), whereas optic atrophy 1 (OPA1) assists inner membrane fusion, which interacts with Mfns and form an intermembrane protein complex that couples the fusion of outer membrane to that of the inner membranes of mitochondria (Olichon *et al.* 2003; Cipolat *et al.* 2004; Song *et al.* 2009).

Fission in turn, involves the recruitment of cytosolic dynamin-related protein 1 (Drp1) and membrane bound fission protein 1 homolog (hFis-1) located on the cytosolic side throughout the outer mitochondria membrane (Figure 3). However, more recently, new outer-membrane proteins involved in fission were identified. Mitochondrial fission factor protein (Mff) (Otera *et al.* 2010) and two homologous proteins Mid49 and Mid51 (also termed MIEF1) (Palmer *et al.* 2011; Zhao *et al.* 2011) serve also as Drp1 receptors. Fission is also thought to be important for mitophagy, where regulation of mitochondrial size by fission if essential for the clearance of this organelle, once inhibition of the division slows down the process (Itoh *et al.* 2013).

Inner mitochondrial membrane fusion seems to have a fundamental prerequisite: the $\Delta\psi_m$. Studies in cell lines have shown that mitochondrial ATP synthesis is unnecessary for fusion, since sufficient glycolytic ATP is available and $\Delta\psi_m$ is maintained (Lombe *et al.* 2002). Fission, in turn, can be linked with large changes in $\Delta\psi_m$. Fission events normally lead to daughter mitochondria with opposite changes in $\Delta\psi_m$ (Twig *et al.* 2008a). The daughter mitochondria with decreased $\Delta\psi_m$ can either manage to reverse this change and reintegrate the fusion apparatus, or are likely to be targeted for degradation by mitophagy, a quality control mechanism (Twig *et al.* 2008b).

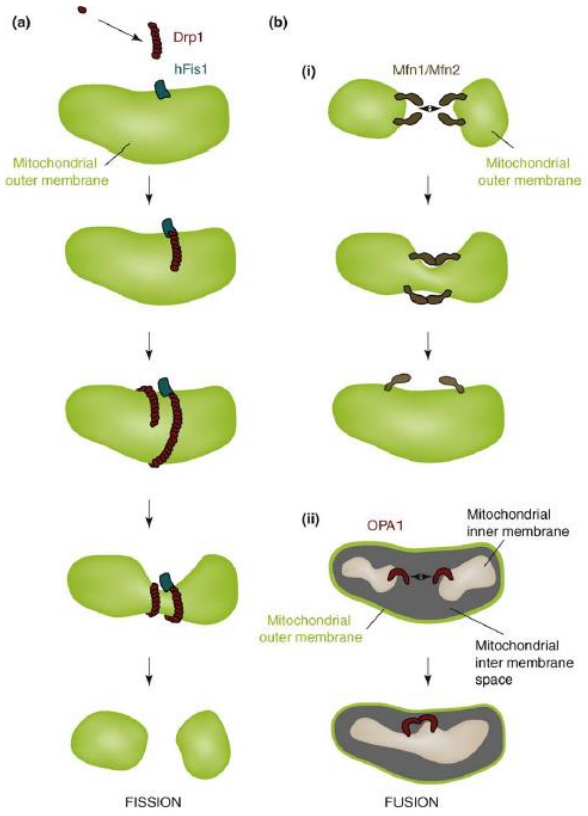

Figure 4: **Mitochondrial fission and fusion (Macaskill & Kittler 2009). (a)** Drp1, which oligomerizes into 8-12 subunit chains, is recruited to mitochondria via the adaptor hFis1. Drp1 oligomerize in spiral chains that wrap around mitochondria. The constriction of Drp1, due GTPase activity, causes mitochondrial fission. **(b)** – (i) *Trans*-dimerization of either Mfn1 or Mfn2 bring into close apposition the membranes of the two mitochondria which are fused due GTPase activity. (ii) Fusion of the inner mitochondrial membrane also involves *trans*-dimerization of OPA1.

1.2. The Presynaptic Compartment of Synapses

Neurons are distinct from many other eukaryotic cells due their unique architecture of the long processes arising from the cell body. Neurons are highly interactive cells whose major function is communication through the neuronal contacts sites, the synapses, where information is received/sent from/to others neurons (Connors & Long 2004; Alonso-Nanclares *et al.* 2008).

It is becoming progressively better documented the important role of synapses in the initiation and progression of many neurodegenerative conditions (Marcello *et al.* 2012;

Picconi *et al.* 2012; Yin *et al.* 2012), leading many to speculate that synapse-specific neuroprotective strategies will be a better approach in order to provide effective therapeutics (Chiesa *et al.* 2005; Koike *et al.* 2008). However, although the knowledge and the increasing awareness of the importance of synapses to the initiation and progression of neurodegeneration, the reason why synapses are so vulnerable to neurodegenerative stimuli remains practically unknown. Understanding of the molecular mechanisms that regulate synaptic degeneration may be a window for the development of synaptoprotective therapies for treating a wide spectrum of neurodegenerative conditions.

Synapses are defined as a physically small structure with an incredible molecularly composition (Gillingwater & Wishart 2013) necessary for the control of a varied range of functions. Gray (1959) recognized two central categories of synapses: the type I or asymmetric synapse (the glutamatergic or excitatory synapses) and the type II or symmetric (GABAergic inhibitory synapses) (Gray 1959). The excitatory synapses are mainly found on dendrites and dendritic spines whereas inhibitory synapses can also be found on the soma and axonal initial segments (Harris & Weinberg 2012). Synapses are sites with only a couple of microns in diameter, containing ion channels and receptors, essential for the control of synaptic function, neurotransmitter-containing synaptic vesicles and a wide range of subsynaptic organelles, such as, mitochondria and endoplasmic reticulum (ER), required for energy supply and newly synthetized proteins. The presynaptic plasma membrane contains one specialized region, the active zone (AZ), characterized by the docking and the preparation of synaptic vesicles for release (Landis *et al.* 1988; Harris & Weinberg 2012). Neurotransmitters are release from docked vesicles into the synaptic cleft and after that the vesicular membranes are recycled via clathrin-mediated endocytosis or via bulk endocytosis, under elevated neuronal activity (Royle & Lagnado 2010; Clayton & Cousin 2009). Importantly, the rise of intra-terminal Ca^{2+} is the main trigger for the coordinated fusion of synaptic vesicles and release of neurotransmitter upon arrival of an action potential to the nerve terminal.

As was already mentioned, enriched mitochondria can be found in locations with high energy demand (Hollenbeck & Saxton 2005), and the presynaptic compartment represent one special location were mitochondria are essential.

1.2.1. Synaptic Vs Non-synaptic Mitochondria

Over the years, numerous studies have demonstrated substantial mitochondrial heterogeneity within the central nervous system (CNS). A typical pattern of mitochondrial heterogeneity is well accepted and regarding their physical position, we may characterize mitochondria as synaptic mitochondria and non-synaptic mitochondria.

In 1989, James Lai and John Clark, demonstrated regional and cellular heterogeneity in the composition, morphology and trafficking of mitochondria (Lai & Clark 1989). Additionally, altered enzymatic activity (Lai *et al.* 1977), ROS production associated with $\Delta\psi_m$ dissipation (Yarana *et al.* 2012) and Ca^{2+} buffering capacities with proceeded or accompanied loss of $\Delta\psi_m$ (Brown *et al.* 2006) were shown to be different between synaptic and non-synaptic mitochondria. Moreover, two other studies have demonstrated different properties of Ca^{2+} handling between both types of mitochondria (Li *et al.* 2004; Guo *et al.* 2005). Furthermore, synaptic mitochondria appear to be more susceptible to surrounding environment. Synaptic mitochondria are exposed to extensive Ca^{2+} fluctuations which may increase the risk for oxidative stress and Ca^{2+} accumulative damage (Martinez *et al.* 1996; Banaclocha *et al.* 1997; Lores-Arnaiz & Bustamante 2011). Additionally, synaptic mitochondria, upon inhibition of ETC complex I, exhibit a more drastic reduction is respiration rates and ATP production when compared with non-synaptic mitochondria (Davey *et al.* 1998).

Synthetized in the cell body of the neuron, synaptic mitochondria, are transported along the axons or dendrites (Morris & Hollenbeck 1993; Ligon & Steward 2000a; Ligon & Steward 2000b). Thus, some have been argued that synaptic mitochondria may be longer lived than mitochondria present in soma of neurons or glial cells, presenting greater cumulative damage from oxidative stress, since aging mitochondria become more heterogeneous and on average, more depolarized (Hagen *et al.* 1997). Accordingly, a

recent work has shown that synaptic mitochondria exhibited increased age-associated mtDNA mutations as well as decreased bioenergetic function compared with non-synaptic mitochondria (Stauch *et al.* 2014).

However, it remains poorly understood why and how synaptic and non-synaptic mitochondria exhibit different properties. It has been suggested that the more limited ability of synaptic mitochondria to buffer Ca^{2+} may be due to the punctuate morphology, differently to the tubular mitochondrial morphology observed in other regions of neurons and glia (Brown *et al.* 2006).

1.2.2. Mitochondria and Synaptic Function

The positioning of mitochondria at synapses fuels several ATP-dependent synaptic processes, such as reversal ion movements following opening of ion channels, exo- and endocytosis in the presynaptic terminal, as well as, refill and reuptake of neurotransmitters. Thus, synaptic ATP depletion, through mitochondrial inhibition, has a dramatic effect on synaptic vesicle turnover and synaptic vesicle release. Indeed, Maxim Ivannikov and colleagues (Ivannikov *et al.* 2013) have shown that variation in the mitochondrial density and/or variation in the rate of mitochondrial oxidative phosphorylation, changes the ability of presynaptically ATP regeneration and, consequently, affects synaptic vesicles exocytosis. They have also shown that synaptosomes with more mitochondria were capable of releasing more synaptic vesicles. Accordingly, Verstreken and colleagues (Verstreken *et al.* 2005) showed an inability to maintain normal neurotransmission during intense stimulation, upon blocking the transport of mitochondria to presynaptic terminals, using Drp1 mutant neurons. Moreover, this effect was partially rescued by application of exogenous ATP, strongly suggesting that ATP provided by mitochondria is essential to fuel myosin-mediated mobilization of reverse pool vesicles. In agreement, it has also been shown the dependence on ATP supply from presynaptic localized mitochondria to fuel the assembly of actin cytoskeleton. The ATP content affects the presynaptic specialization including the

clustering of synaptic vesicles and mitochondria (Lee & Peng 2008), as well as the efficient mobilization of synaptic vesicles into the readily releasable pool (Ma *et al.* 2009).

Furthermore, mitochondria through cytosolic Ca^{2+} uptake, offer an additional dimension for synaptic release. Over stimulation, large intracellular Ca^{2+} rises occur in the presynaptic compartment, mainly to act locally and to facilitate vesicle fusion or to influence many signaling cascades. Mitochondria, thanks to the negative membrane potential created via the ETC along with plasma membrane Ca^{2+}-ATPases and the ER, modulate these process by regulating Ca^{2+} levels (Rizzuto 2001; Rizzuto *et al.* 2004). Indeed, several studies regarding the buffering of Ca^{2+} by mitochondria at the synapse have been published. Using mouse motor nerve terminals, it was observed that during repetitive stimulation, mitochondrial Ca^{2+} uptake protect the terminals from synaptic rundown and asynchronous firing, by limiting the rise in $[Ca^{2+}]_c$ (David & Barrett 2003). In another study, using drugs that either disrupt the mitochondrial potential (i.e., antimycin or CCCP [carbonyl cyanide chlorophenyl hydrazine]) or inhibit the calcium uniporter (i.e., ruthenium red), Tang and Zucker (1997) observed rises in $[Ca^{2+}]_c$ over repetitive stimulation (Tang & Zucker 1997). Moreover, evaluation of the blockage of both Na^+-dependent and independent mitochondrial Ca^{2+} efflux by using tetraphenylphosphonium (TPP^+), has shown that synaptic strengthening required a slow release of Ca^{2+} from mitochondria (Tang & Zucker 1997).

Furthermore, Kang and colleagues (Kang *et al.* 2008) tested, in rat hippocampal presynaptic terminals, the effect of depletion of mitochondria by ablating the axon-targeted syntaphilin or by uncoupling $\Delta\psi_m$. They observed an enhanced short-term facilitation over prolonged synaptic stimulation. As expected from the key role of Ca^{2+} accumulation in the nerve terminal for the expression of paire-pulse facilitation.

Effects on synaptic function and degeneration, as well as on structural remodeling, can be triggered locally by apoptotic cascades. Prostate apoptosis response 4 (Par-4), which is locally induced at the translational level within synaptic terminals subjected to apoptotic stimuli, can cause changes in $\Delta\psi_m$ and oxyradicals production. On the other hand, p53, which has been shown to be present at synapses, can be activated and induce

mitochondrial membrane permeability (Gilman & Mattson 2002). Additionally, Mattson and colleagues (Mattson *et al.* 1998b) showed that exposure of synaptosomes to apoptotic triggers can result in loss of membrane phospholipid asymmetry, mitochondrial membrane depolarization, ROS production, Ca^{2+} overload and activation of caspase 3. Therefore, it can be argued that "synaptic apoptosis" can indeed occur, being independent of the cell body apoptosis and thereby playing a role in synaptic remodeling or synaptic loss.

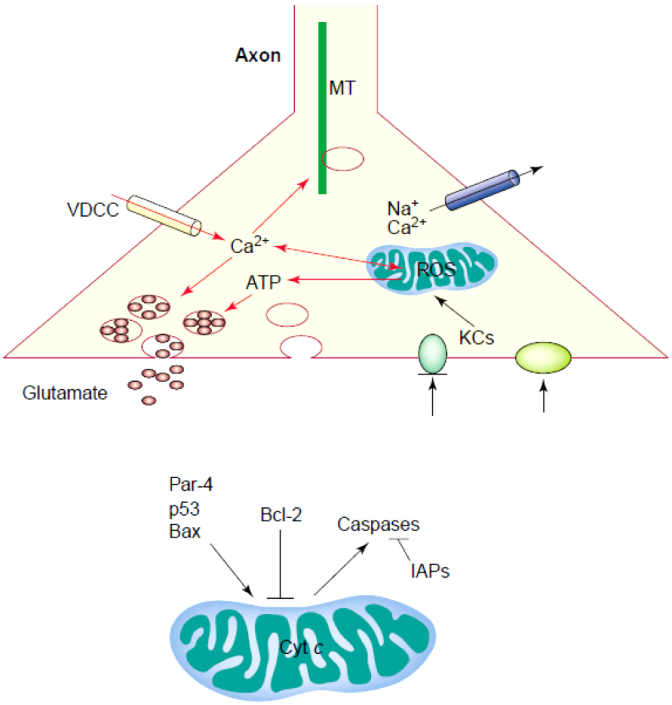

Figure 5: Apoptosis at distance (adapted from (Mattson & Kroemer 2003): roles of mitochondria in degeneration and cell death propagation. Presynaptic terminals: mitochondria by producing ATP and ROS as well as by modulating intracellular Ca^{2+} levels as a key role on neurotransmitter (e.g. glutamate) release, vesicle recycling, ion homeostasis (mainly Na^{+} and Ca^{2+}) and cytoskeleton dynamics. Abbreviations: CSK, cytoskeleton (actin filaments); Cyt c, cytochrome c; GR, glutamate receptors; IAPs, inhibitor apoptosis proteins; KCs, kinase cascades; MT, microtubules; Par-4, prostate apoptosis response 4; TF, transcription factor; VDCC, voltage-dependent calcium channel.

1.3. Alzheimer's Disease

Alzheimer's disease, a devastating neurodegenerative disorder, affects ~6% of both North Americans and Europeans above the age of 60, and over 25% above the age of 85 (McInnes 2013). There are two types of AD: the majority of cases are sporadic but it is estimated that 1-5% of the cases carry genetic mutations in amyloid precursor protein (APP), presenilin1 (PS1) and presenilin2 (PS2) that are thought to contribute to the early-onset of the disease (Reddy & Beal 2008).

Clinically, AD is characterized by a progressive impairment of memory accompanied by cognitive disabilities, such as personality changes and in the late stages, complete dependence on others. Histopathologically, AD is traditionally characterized by two major hallmarks: abnormal processing and accumulation of Aβ, cleaved from the transmembrane APP, followed by the accumulation of intraneuronal neurofibrillary tangles (NFTs) of hyperphosphorylated microtubule-associated protein tau (Goedert & Spillantini 2006). Although the cause of AD still remains to be identified, the levels of soluble Aβ, mainly $A\beta_{1-42}$ have been reported as the best neurochemical parameter correlated with early memory dysfunction in AD (Selkoe 2001; Hardy & Selkoe 2002). Progressive synaptic loss and consequently death of neurons in brain regions critical for learning and memory process, such as the hippocampus (Coleman *et al.* 2004), mitochondrial structural and functional abnormalities, and inflammatory responses are all characteristics of AD (Reddy 2011).

Aβ is generated from the proteolytic cleavage of APP in neurons, with $A\beta_{1-40}$ and $A\beta_{1-42}$ being the dominant species produced (Kang *et al.* 1987). APP processing occurs by the action of integral membrane proteases termed secretases (Haass & Selkoe 2007). Two pathways are designed from Aβ processing: the amyloidogenic pathway where APP experiences sequential proteolysis first by α- or β-secretases and then by γ-secretases, which result on the production of Aβ peptides, and the non-amyloidogenic pathway where cleavages occur by α-secretases within Aβ domain preventing the formation of full Aβ (Hemachandra & Flint 2008) (Figure 6). Thus, in the amyloidogenic pathway, intramembranous cleavage by γ-secretases is responsible for the production of Aβ

peptide, where the more hydrophobic, aggregation-prone $A\beta_{1-42}$ is believed to be more neurotoxic than $A\beta_{1-40}$ and others Aβ variants (Sheng *et al.* 2012).

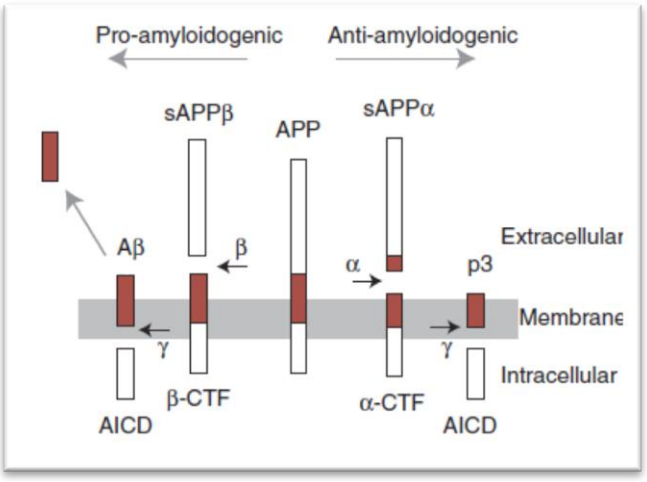

Figure 6: APP processing and formation of Aβ peptide (adapted from (Sheng *et al.* 2012)): In the middle is represented the full-length human amyloid precursor protein (APP), a single transmembrane protein with a carboxyl terminus present intracellularly. Specific proteases cleavage sites are represented by the horizontal arrows. In the amyloidogenic pathway, β-secretases and γ-secretases cleave APP releasing soluble extracellular domain of APP (sAPPβ), Aβ peptide, and the intracellular carboxyl-terminal domain of APP (AICD). The activity of α-Secretases prevents the formation of Aβ peptide, producing sAPPα and p3 peptide. (CTF) represents the carboxyl-terminal fragment of APP, before cleavage by γ-secretase.

1.3.1. Alzheimer's Disease is a Synaptic Failure

The idea that researchers must focus their clinicopathological analysis on early stages of the disease has become clear over the years. Studying the brains of individuals dying, for any other reason, with very subtle memory deficits that often is the harboring of AD, is more likely to yield convincing mechanistic and therapeutic insights than studying the late-onset AD brains. Loss of whole neuron matters, but matters less than synaptic loss in the early phases of AD (Selkoe 2002). Already in 1991, Robert Terry and colleagues have reported synapse loss as a major correlate of cognitive dysfunction (Terry *et al.* 1991). These results indicated that synaptic loss correlated better with memory impairment in AD patients than are the number of Aβ plaques, NFTs, neuronal loss or the extent of

cortical gliosis (Selkoe 2002). Furthermore, several studies on synaptic proteins have also been reported. Compared to age-matched control subjects, AD patients display decreased levels of synaptophysin, a presynaptic protein (Hemachandra & Flint 2008), suggesting that presynaptic proteins are involved in AD progression and that synapses may be the brain compartment initially affected in AD (Hemachandra & Flint 2008).

Accordantly, the loss of synapses (Scheff *et al.* 1990; Scheff *et al.* 2006), as well as the loss of synaptic markers (Masliah *et al.* 1989; Sze *et al.* 2000) has been documented in early AD, and in different animal models of AD (Richardson *et al.* 2003; Canas *et al.* 2009). Additionally, the first direct association between Aβ peptide and synapse pathology in the brain was reported by Takahashi and colleagues (Takahashi *et al.* 2002) where they observed an aberrant accumulation of $A\beta_{1\text{-}42}$ on synapses. Moreover, interesting evidences have been reported showing a modulation of Aβ homeostasis by synaptic activity (Kamenetz *et al.* 2003; Cirrito *et al.* 2005; Cirrito *et al.* 2008). These discoveries appear to fit with the hypothesis that brain areas with highest synaptic activity, such as hippocampus, are most vulnerable to early AD pathology (Buckner *et al.* 2005). Thus, increased Aβ secretion induced by synaptic activity could lead to the damage and loss of synapses and consequently, leads to accumulation of extracellular Aβ into amyloid plaques, an important hallmark of AD. Furthermore, intraneuronal Aβ accumulation has been also associated with the pre-plaque onset of both physiological and behavioral anomalies in AD transgenic models (Echeverria *et al.* 2004; Billings *et al.* 2005; Knobloch *et al.* 2007). Clearance of intraneuronal Aβ by treatment with Aβ antibodies has been correlated with memory improvement (Billings *et al.* 2005) and protection of synapses (Tampellini *et al.* 2007).

Moreover, Tampellini and colleagues (Tampellini *et al.* 2009) have shown that, with synaptic activation, APP is anterogradely transported to synapses, followed by internalization and amyloidogenic processing at active synapses. Thus, increase APP anterogradely transported and β-cleavage throughout synaptic activity, support that Aβ production is locally enhanced at activated synapses (Cirrito *et al.* 2008; Tampellini *et al.* 2009). Furthermore, cumulative evidence supports a scenario where the accumulation of

intraneuronal $A\beta_{1-42}$ at early stages of AD, occurs gradually within synapses, affecting normal synapse function. Consequently, following degeneration of the synapses, intraneuronal $A\beta_{1-42}$ is released in the extracellular space contributing to toxic spread of Aβ pathology to surrounding synapses (Tampellini & Gouras 2010).

Additionally, the particular susceptibility of glutamatergic synapses in early AD has been reported by our group. Diana Rodrigues and colleagues (Rodrigues *et al.* 2014) have shown that APP is predominantly distributed among glutamatergic terminals rather than GABAergic and cholinergic terminals. In line with this findings, Paula Canas and colleagues (Canas *et al.* 2014) have also reported a predominant susceptibility of glutamatergic synapses in an Aβ-model of AD. Still, it remains to be elucidated why and how only some particular synapses, namely limbic cortical glutamatergic synapses (Bell *et al.* 2003; Kirvell *et al.* 2006; Kashani *et al.* 2008; Canas *et al.* 2014), are more prone to begin degeneration in AD.

1.3.2. Synaptic Mitochondria Failure in Alzheimer's Disease

Mitochondrial dysfunction has been recognized as a predominant AD pathological change. However, increasing evidences suggest that mitochondrial dysfunction may occur in parallel with synaptic alterations exacerbating disease progression. Indeed, Xiao-Liang Zhao and colleagues (Zhao *et al.* 2010) have shown that $A\beta_{1-42}$ can accumulate intracellularly and induce a range of age-dependent changes, including depletion of presynaptic mitochondria. Concerning this and based on the critical role of synaptic mitochondria in sustaining synaptic activity, the mechanisms that drive synaptic mitochondria dysfunction as a potential player in synaptic failure in AD represent the focus of many researchers in the last years.

Actually, several studies have revealed that Aβ accumulates inside the mitochondria in the AD brain, as well as on synaptic mitochondria, and that these levels of mitochondrial Aβ are linked to abnormalities of both mitochondrial structure and function. Decreased ATP provision, elevated mitochondria-associated oxidative stress, increased mitochondrial permeability transition, reduced mitochondrial Ca^{2+} modulating

capacity, impaired respiratory function and release of pro-apoptotic factors are the most recognized forms of mitochondrial dysfunction in AD (Du *et al.* 2012). Thus, finding the type of changes that occur in the synaptic compartments becomes more imperative in AD, and mitochondrial dysfunction has become a progressive branch of interest.

Acordingly, Mungarro-menchaca and colleagues (Mungarro-menchaca *et al.* 2002), using a synaptosomal preparation, observed a potentiation of mitochondrial dysfunction by $A\beta_{25-35}$ peptide, diminishing the overall capacity of ETC and inducing morphological changes resulting in mitochondrial swelling. In another study, the same $A\beta_{25-35}$ peptide as well the $A\beta_{1-42}$ peptide, showed a propensity to induce mitochondrial membrane depolarization in synaptosomal preparations (Mattson *et al.* 1998b). Additionally, another synaptosomal preparation used in an *in vitro* experiment demonstrated striking changes of synaptic mitochondria, including membrane potential collapse, mitochondrial calcium accumulation, and increased free radical production after treatment of synaptosomes with $A\beta_{1–40}$ peptide (Keller *et al.* 2000). Furthermore, *in vivo* experiments using AD animal models have also suggest the existence of Aβ-induced pathogenesis in synaptosomes (Gillardon *et al.* 2007). Alteration of mitochondrial proteome and function were observed before amyloid plaque deposition suggesting-mitochondria as an early target of β-amyloid aggregates (Gillardon *et al.* 2007). Supporting this idea, another study showed, in an AD mouse model, that the levels of both Aβ species used in the experiment ($A\beta_{1-40}$ and $A\beta_{1-42}$) were increased in synaptic mitochondria when compared with non-synaptic mitochondria (Du *et al.* 2010). As a result, synaptic mitochondria undergo significant decline in respiratory function and cytochrome c oxidase activity, increased oxidative stress, and enhanced probability of mitochondrial permeability transition pore. These results confirm that synaptic mitochondria are more vulnerable to Aβ accumulation than non-synaptic mitochondria suggesting that Aβ aggregation in synaptic mitochondria is an early mitochondrial process in Aβ pathology. Familial forms of AD have also been studied regarding the alteration of synaptic mitochondria. Using transgenic mice harboring presenilin-1 mutations, synaptosomal preparations exhibit mitochondrial dysfunction and

caspase activation following exposures to β-amyloid peptide due perturbed Ca^{2+} homeostasis; apoptotic cascade events were also activated (Begley *et al.* 1999).

Over the years Aβ has been well accepted to be a causative factor underlying AD pathogenesis leading to mitochondria deficits. However, some doubts have arisen, questioning whether Aβ is produced in mitochondria or reaches mitochondria from other subcellular locations. Interesting, Camilla Hansson and colleagues (Hansson *et al.* 2004) identified the γ-secretase complex within mitochondria, showing that these complex indeed could cleave β-APP. Still, β-APP have already been identified to be located in the mitochondrial membranes (Anandatheerthavarada *et al.* 2003), however, this insertion is incomplete and appears to be different compared with other membranes. β-APP was found in an N-in C-out orientation spanning the mitochondrial intermembranar space in contact with mitochondrial inner and outer translocase proteins, being suggested that a 22-kDa region (N-terminal) of β-APP is located inside mitochondria membrane and that the remaining 73-kDa portion, containing the Aβ sequence and γ-secretase cleavage site (C-terminal), faces the cytoplasmic site (Anandatheerthavarada *et al.* 2003). These conclusions brought new issues, leading some to suggest that, if indeed the orientation of β-APP is correct, β-APP may not be a substrate for mitochondrial γ-secretase since Aβ region is located in the intermembrane space (Anandatheerthavarada *et al.* 2003) and γ-secretase complex is an intramembranous cleavage protease (Haass & Steiner 2002; Wolfe & Kopan 2004). Furthermore, it was also shown that Aβ may interact with mitochondrial matrix proteins. Aβ-insulted synaptic mitochondria also showed increased expression of CypD (increase vulnerability to mitochondrial permeability transition) and Aβ-binding alcohol dehydrogenase (ABAD) (Takuma *et al.* 2005; Yan & Stern 2005; Naga *et al.* 2007).

Regarding this information, it seems recognizable that a lack of full characterization of both normal synaptic mitochondria as well as synaptic mitochondria from AD patients or animal models of AD is missing. Elucidation of mitochondrial parameters relevant for their function in individual synaptic compartments, namely $\Delta\psi_m$, will provide knowledge to develop attractive therapeutic intervention to manage AD.

2.AIM

This work will focus on two main objectives:

- **Optimization of a protocol to assess *in situ* mitochondria membrane potential in purified nerve terminals;**
    - To achieve this goal we will start by isolating presynaptic nerve terminals through a discontinuous Percoll gradient. These nerve terminals are plated on gridded coverslips and analyzed through live imaging experiments with a mitochondrial fluorescent probe;

- **Assess if presynaptic mitochondria located in glutamatergic nerve terminals are particularly affected in an $A\beta_{1-42}$ *in vitro* model;**
    - After live imaging, purified nerve terminals are subjected to an immunocytochemistry assay labeling mitochondria (Tom20) and glutamatergic nerve terminals (VGLUT1), which will allow identifying mitochondrial changes selectively occurring in glutamatergic terminals.

3. MATERIAL AND METHODS

3.1. Materials

3.1.1. Reagents

Table 1: reagents used

Reagent	Supplier
Boric acid	Sigma-Aldrich (Portugal)
Bovine serum albumin (BSA)	Sigma-Aldrich (Portugal)
Calcium Chloride ($CaCl_2$)	Sigma-Aldrich (Portugal)
Cyanide *p*-trifluoromethoxy)phenylhydrazone) (FCCP)	Sigma-Aldrich (Portugal)
Dimethylsulfoxide (DMSO)	Sigma-Aldrich (Portugal)
Dithiothreitol (DTT)	Sigma-Aldrich (Portugal)
Ethanol (EtOH)	Ensure / Merck
Ethylenediaminetetraacetic acid, disodium dihydrate ($EDTA.Na_2.2H_2O$)	Sigma-Aldrich (Portugal)
Glucose	Sigma-Aldrich (Portugal)
Glycerol	Sigma-Aldrich (Portugal)
2-Bromo-2-chloro-1,1,1-triflouroethane (Halothane)	Sigma-Aldrich (Portugal)
2-[4-(2-hydroxyethyl)piperazin-1-yl]ethanesulfonic acid (HEPES)	Sigma-Aldrich (Portugal)
Magnesium chloride ($MgCl_2$)	Sigma-Aldrich (Portugal)
Normal horse serum (NHS)	Invitrogen (United Kingdom)
Oligomycin	Sigma-Aldrich (Portugal)
Paraformaldehyde	Sigma-Aldrich (Portugal)
Percoll	GE Healthcare (United Kingdom)
Plasma membrane potential indicator (PMPI)	Molecular Devices
Poli-D-Lysine	Sigma-Aldrich (Portugal)
Potassium chloride (KCl)	Sigma-Aldrich (Portugal)
ProLong Gold Antifade	Invitrogen (United Kingdom)
Sodium bicarbonate ($NaHCO_3$)	Sigma-Aldrich (Portugal)
Sodium chloride ($NaCl_2$)	Sigma-Aldrich (Portugal)
Sodium phosphate monobasic monohydrate ($NaH_2PO_4.H_2O$)	Sigma-Aldrich (Portugal)
Sucrose	Sigma-Aldrich (Portugal)
Tetramethyl rhodamine methyl ester (TMRM)	Invitrogen
Triton X-100	Sigma-Aldrich (Portugal)

Phosphate buffered saline (PBS)	Sigma-Aldrich (Portugal)
Trizma base	Sigma-Aldrich (Portugal)

3.1.2. Antibodies

Table 2: Primary and secondary antibodies for immunocytochemistry

Antibody	Supplier	Host	Type	Dilution
VGLUT1	Synaptic systems	Guinea pig	Polyclonal	1:2000
Tom20	Santa Cruz	Rabbit	Polyclonal	1:1000
Anti-Guinea pig Alexa Fluor 594	Invitrogen	Goat	IgG (H+L)	1:1000
Anti-rabbit Alexa Fluor 647	Invitrogen	Goat	IgG (H+L)	1:2000

3.1.3. Animals

Adult male wistar rats (8-10 weeks) were obtained from Charles River (Barcelona, Spain) and were maintained at 23-25 ^{o}C, with 12h light – 12h dark, with food *ad libitum*. The study was conducted in accordance with the principles and procedures outlined as "3 Rs" in the guidelines of European Union (Directive 2010/63/EU).

3.2. Methods:

3.2.1. Synaptosomal preparation

Nerve terminals can be separated from their axons, postsynaptic connections as well as glial cells to which they are connected, through homogenization of fresh brain in isotonic medium where presynaptic membranes can reseal to form synaptosomes (Dunkley *et al.* 2008).

Synaptosomes contain all the expected neuronal contents, including cytoplasm, synaptic vesicles, mitochondria and cytoskeleton, that closely mimics nerve terminals *in vivo*: they can produce ATP, they can have functional ion channels, carriers and receptors responsible by the maintenance of membrane potential and ion homeostasis, as well as functional proteins, enzymes and synaptic vesicles capable of taking up and release neurotransmitters (Dunkley *et al.* 2008). With appropriated nutrients, it is possible to study physiological properties of synapses for several hours (Whittaker 1993).

3.2.1.1. Purification of nerve terminals with a discontinuous Percoll gradient

For the *in situ* experiments and for the immunochemical assays in purified nerve terminals, purified nerve terminals were obtained through a discontinuous Percoll gradient as previous described (Dunkley *et al.* 1986; Dunkley *et al.* 2008). Nevertheless, it is important distinguish purified nerve terminals from synaptosomes since it is not indifferent speak of synaptosomes or purified nerve terminals. Purified nerve terminals practically only have a presynaptic component of the synapse whereas synaptosomes by definition are a fraction of synapses, which present both the pre- and postsynaptic components. This procedure for preparation of purified nerve terminals allowed us to reduce the amount of postsynaptic density material, as showed previously (Díaz-Hernández *et al.* 2002), with less than 1% of synaptophysin-positive elements also immunopositive for postsynaptic density protein 95 (PSD-95). This was particularly

important for our immunochemical assays in purified nerve terminals, since our goal was to identify mitochondria in presynaptic glutamatergic nerve terminals.

The first step in this procedure was the preparation of Percoll solutions. The Percoll solution were prepared in a 0.32 M sucrose solution with 1 mM $EDTA.Na_2.2H_2O$, 5 mM Tris and 0.25 mM dithiothreitol (DTT), pH 7.4 at 4 ºC. In each tube, the gradient was built as follows (from bottom to top): 3 mL of a 23% (v/v) Percoll solution, 5 mL of a 10 % (v/v) Percoll solution and 3 mL of a 3% (v/v) Percoll solution (Figure 7).

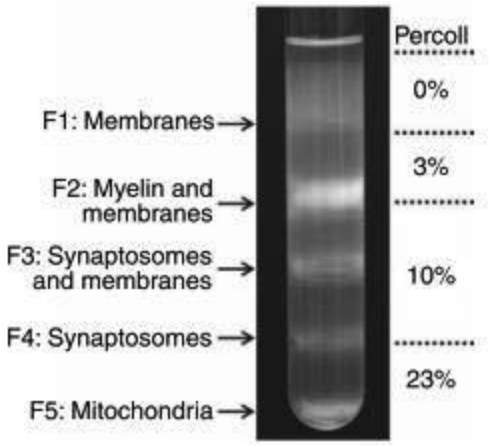

Figure 7: Representation of a discontinuous Percoll gradient (adapted from Dunkley *et al.* 2008).

The animals were anesthetized under saturated halothane atmosphere (1 mL) before being sacrificed by decapitation. The two hippocampi from one male rat were homogenized at 4 ^{o}C in 10 volumes of a 0.25 M sucrose solution (containing: 0.25 M sucrose and 10 mM HEPES, pH 7.4), 10/12 strokes. The homogenate was centrifuged at 2000 x*g* for 3 min at 4 ^{o}C (Sigma 3-18K centrifuge, rotor 12- 158H) and then the supernatant was collected and centrifuged at 9500 x*g* for 13 min at 4 ^{o}C (Sigma 3-18K centrifuge, rotor 12- 158H). The supernatant was discarded and the pellet was ressuspend in 2 mL of 0.25M sucrose solution. This suspension was slowly and carefully placed over the top 3% layer in the tube containing the Percoll discontinuous gradient prepared in

advance. These gradients were then centrifuged at 25000 x*g* for 11 min at 4 ^{o}C, without deceleration.

Purified nerve terminals were collect between the 10% (v/v) and 23% (v/v) Percoll interface and diluted in 10 mL of HEPES buffered medium (HBM, containing: 140 mM NaCl, 5 mM KCl, 1.2 mM NaH_2PO_4, 5 mM $NaHCO_3$, 10 mM glucose, 10 mM HEPES and 1.2 mM $MgCl_2$, pH 7.4). After that, purified nerve terminals were centrifuged at 22000 x*g* for 11 min at 4 ^{o}C and the resulting freely-moving pellets were carefully removed, ressuspended in HBM, and centrifuged at 11000 x*g* for 11 min at 4 ^{o}C. Finally, and dependent on the volume of animal tissue obtained, the purified nerve terminals were ressuspended again in HBM, to achieve an optical density between 0.055-0.057 at 600 nm, for the plating.

3.2.2. Live imaging experiments

3.2.2.1. Assessment of mitochondrial and plasma membrane potential:

The hippocampal nerve terminals obtained through a discontinuous Percoll gradient were plated on 12 mm gridded coverslips (Bellco biotechnology, New Jersey, USA) coated with poly-D-lysine for 45 min at room temperature (RT). The purified nerve terminals were incubated in HEPES buffered medium supplemented with 1.2 mM $CaCl_2$ in the presence or absence of soluble $A\beta_{1-42}$ (500 nM) as previously used by the group (Canas *et al.* 2009), followed by a 30 min incubation of 7.5 nM tetramethyl rhodamine methyl ester ($TMRM^+$), a mitochondrial membrane-permeable fluorescent dye, or 1 µL/mL PMPI stock at RT in the dark. The PMPI concentration was prepared as previously described (Nicholls 2006), corresponding to a 1:2000 dilution of a PMPI stock dilution where one R-8042 Component A vial was reconstituted in 1 mL of ultrapure water.

After the incubation, the coverslips were placed in a perfusion chamber (RC-20; Warner Instruments, Harvard, UK), with 500 µL of incubation medium, on the stage of an inverted fluorescence microscope (Axiovert 200; Carl Zeiss, Jena, Germany). Purified nerve terminals were alternately excited at 550 ± 10 nm using an optical splitter (Lambda DG4;

Sutter Instruments, Novato, CA, USA), and the emitted fluorescence was captured at 600 ± 20 nm through a 100× oil objective connected to a digital camera (CoolSNAP; Roper Scientific, Trenton, NJ, USA). Acquired images were processed using MetaFluor software (Universal Imaging Corp., Buckinghamshire, UK). The masks of individual purified nerve terminals were drawn, and the average value of pixel intensities was evaluated at each time point. Image acquisition was performed during 500 milliseconds every 30 seconds for a total of 10 minutes. All the compounds tested were prepared in a HBM buffer medium supplemented with 1.2 mM $CaCl_2$ and added to the purified nerve terminals directly into the bath with a pipette. The recording started by establishing an initial baseline for 2.5 minutes followed by a simultaneously addition of 5 µL of a cocktail of cyanide *p*-(trifluoromethoxy)phenylhydrazone (FCCP) (1 mM) and oligomycin (1mg/mL) (10:1 respectively) that will establish a final baseline during 7.5 minutes. The effect of tested drug was measured as the difference between the final and initial values and is expressed as the percentage of difference observed in control conditions. The protonophore FCCP, which is widely employed to depolarize mitochondria, was combined with application of ATP-synthase inhibitor oligomycin to prevent ATP depletion via the reverse mode of synthase (Nicholls & Ward 2000).

Additionally, different types of controls were also performed. The photobleaching of the dye was measured, were the signal of the dye was acquired during the experiment time (10 min) without any stimuli. Additionally, an experiment where the vehicle of the cocktail of oligomycin and FCCP, absolute ethanol (EtOH), was added at 2.5 minutes to confirm that the response was not due the vehicle of the stimuli. Finally, mitochondrial and plasma depolarization was also assessed by addition of 30 mM KCl at 2.5 minutes.

The presentations of representative traces of the changes of fluorescence in the purified nerve terminals were subjected to standardization. As shown in figure 8A, the initial fluorescence intensity varies between purified nerve terminals incubated in the absence or presence of 500 nM $A\beta_{1-42}$, as well as between different purified nerve terminals in the same condition. Since our aim was to compare the difference between

fluorescence responses in different conditions, we normalized the fluorescence traces in relation to the first value of fluorescence, as presented in figure 8B.

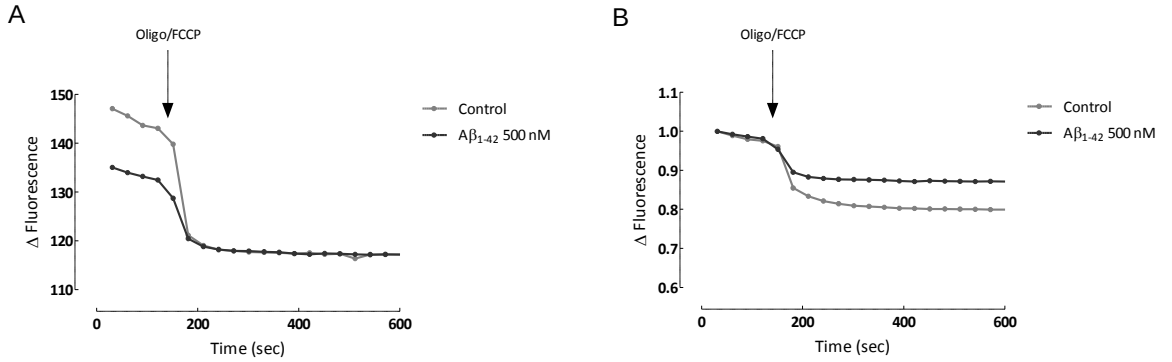

Figure 8: Normalization of purified nerve terminals fluorescence. (A) Representative traces of the fluorescence of plated purified nerve terminals incubated for 2 h in the absence or presence of 500 nM $A\beta_{1-42}$ in HBM medium supplemented with 1.2 mM $CaCl_2$ following 30 min of incubation with 7.5 nM $TMRM^+$. A cocktail of oligomycin (9 µg/mL) and FCCP (9 µM) was added at 2.5 minutes to collapse $\Delta\psi_m$. (B) Representative traces of the fluorescence, normalized in relation of first value, of plated purified nerve terminals incubated for 2 h in the absence or presence of 500 nM $A\beta_{1-42}$ in HBM medium supplemented with 1.2 mM $CaCl_2$ following 30 min of incubation with 7.5 nM $TMRM^+$. A cocktail of oligomycin (9 µg/mL) and FCCP (9 µM) was added at 2.5 minutes to collapse $\Delta\psi_m$. From now on, the representative data will be presented always normalized in relation of first value.

3.2.3. Immunocytochemistry in purified nerve terminals

The purified nerve terminals used for live imaging experiments were subsequently fixed with 4% paraformaldehyde in phosphate buffered saline (PBS), pH 7.4 at 4 ^oC for 15 min and washed twice with PBS (containing: 140 mM NaCl, 3 mM KCl, 20 mM NaH_2PO_4 and 15 mM KH_2PO_4), pH 7.4 at 4 ^oC. The purified nerve terminals were permeabilized using PBS with 0.2% Triton X-100 for 10 min at RT, and then blocked with PBS containing 3% bovine serum albumin (BSA) and 5% normal horse serum (NHS) for 1h to prevent non-specific binding. After that, the purified nerve terminals were washed twice in PBS in the presence of 3% BSA and incubated with primary antibodies against the vesicular

glutamate transporters (VGLUT1 1:2000) and against the mitochondrial preprotein translocases of the outer membrane (Tom20 1:1000) in PBS with 3% BSA for 1h at RT. They were then washed three times with PBS with 3% BSA and immunolabeled with two Alexa Flour conjugates: Alexa Fluor 594-conjugated goat anti-guinea pig (1:1000, Invitrogen) and Alexa Fluor 647-conjugated goat anti-rabbit (1:2000, Invitrogen) for 1h at RT. After the incubation with the secondary antibodies, the purified nerve terminals were washed three times in PBS medium, mounted on glass slides with Prolong Antifade and left to dry overnight. It was confirmed that none of the secondary antibodies produced any signal in preparations to which the addition of the corresponding primary antibody was omitted. The preparations were then visualized by fluorescence microscopy (Zeiss Axiovert 200 microscope with a 63× oil objective), under a total magnification of 630 times.

3.2.4. Identification of glutamatergic nerve terminals

For co-localization purposes, the identification of glutamatergic nerve terminals in each gridded coverslip was carried out by immunocytochemical labeling with glutamatergic terminal marker analyzed using Fiji (Image J) software.

The first step in this analysis was the acquisition of different images using the single-cell calcium imaging microscope. We start by acquiring an image only with the transmission field, which allowed identifying all the elements present in the gridded coverslip (Figure 9A; we then acquired, in the same field, the emission of fluorescence of $TMRM^+$ to allow identifying the individual functional nerve terminals and draw masks of these individual nerve terminals (Figure 9B); we then proceeded to carry out the functional assays. After the immunocytochemical staining with the presynaptic marker, we could re-identify the individual nerve terminals thanks to their position in the gridded coverslip. We then acquired the final image corresponding to the labeling of VGLUT1 and Tom20. Using Fiji (Image J) software we can co-localize the labeling to VGLUT1 and Tom20 (Figure 9C) in order to identify if the nerve terminals draw (B) are glutamatergic or not.

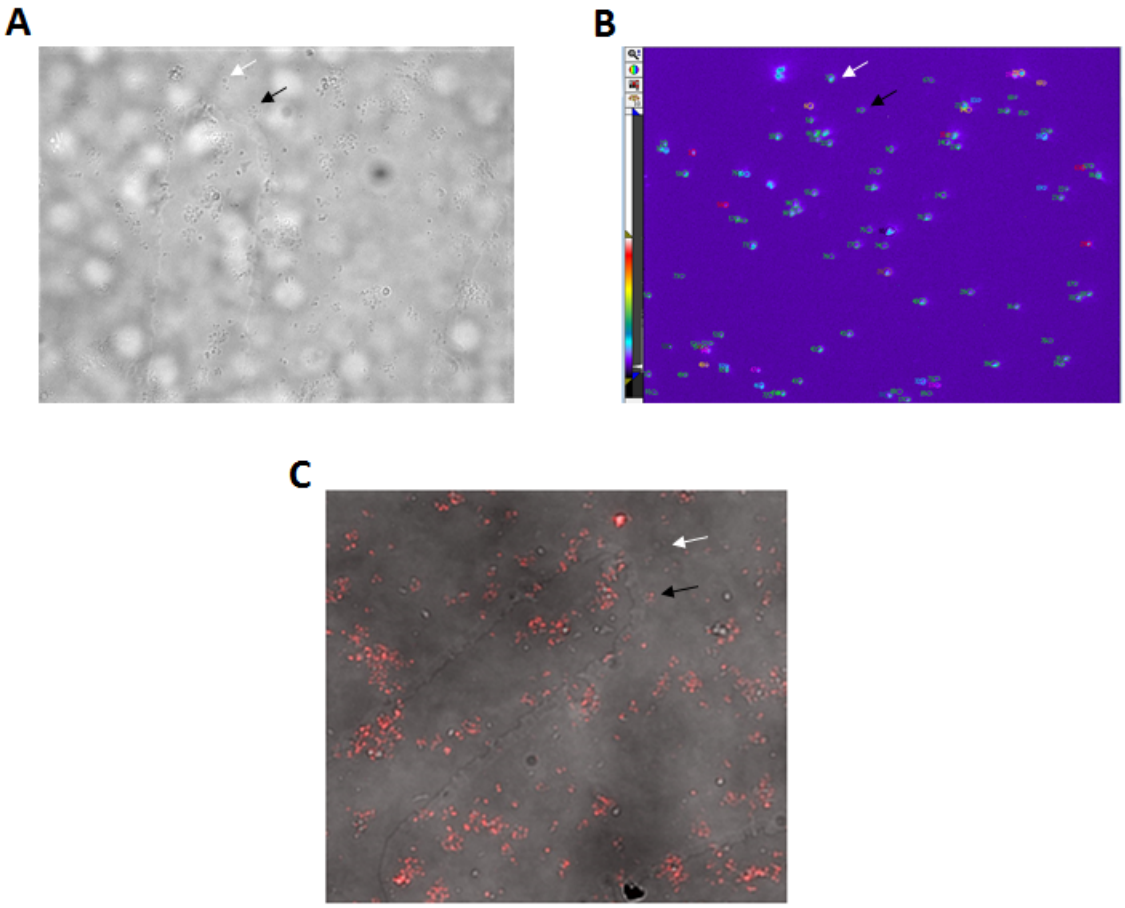

Figure 9: Identification of glutamatergic nerve terminals. (A) Representative transmission image identifying all the elements in this field in the gridded coverslip before the *in situ functional* experiments. (B) Representative images of the fluorescence pattern of $TMRM^{+}$-labelled nerve terminals, which allows drawing masks to identify functional nerve terminals in subsequent analyses. (C) Representative images of the same field of nerve terminals after the functional *in situ* experiments and subsequent immunocytochemistry labeling with VGLUT1. Images in A and B are acquired with a 100× oil objective and images in C are acquired with a 63× oil objective. The back arrow identifies a VGLUT1-immunopositive element (C), corresponding to a glutamatergic nerve terminal. The white arrow identifies a no VGLUT1-immunonegative element (C), corresponding to a non-glutamatergic nerve terminal.

3.2.5. Data presentation

Results are presented as mean ± Standard Error of the Mean (S.E.M.) values of the number of experiments (n) indicated in legend to the figures. To test the significance of the differences between groups, a paired Student's *t*-test was used considering a statistical difference of $p < 0.05$.

4. RESULTS

Rationale

Since *in situ* mitochondria cannot be accessed directly, indirect methods, which predominantly use membrane-permeable cationic fluorescent dyes, have become commonly used to monitor $\Delta\psi_m$ (Nicholls & Ward 2000). As these dyes are cationic compounds that equilibrate across membranes in a Nernstian fashion, they accumulate into the mitochondrial matrix space in a manner inversely proportional to the $\Delta\psi_m$ (Johnson *et al.* 1981; Lemasters & Ramshesh 2007; Ehrenberg *et al.* 1988; Nicholls & Ward 2000). Therefore, more polarized mitochondria (i.e. the interior is more negative, hyperpolarized) will accumulate more cationic dye, and depolarized mitochondria (i.e. interior is less negative) accumulate less dye.

Fluorescent lipophilic cationic dyes, such as tetramethylrhodamine methyl (TMRM) and ethyl (TMRE) ester, Rhodamine 123 (Rhod123), 3,3′-dihexyloxacarbocyanine iodide (DiOC6) and 5,5′,6,6′-tetrachloro-1,1′,3,3′-tetraethylbenzimidazolylcarbocyanine iodide (JC-1) have become important tools to measure $\Delta\psi_m$ and their characteristics and usage paradigms have been elucidated (Perry *et al.* 2011).

For our experiments, we have decided to use $TMRM^+$ because it exhibits: i) low mitochondrial binding and ETC inhibition, ii) a fast equilibrium with mitochondrial matrix and iii) a better profile for non-quenching studies (see below) thanks to its fast equilibrium kinetics.

4.1. Quenching detection limit of $TMRM^+$ in the mitochondrial matrix of purified nerve terminals

In situ experiments on any type of cells loaded with membrane potential probes, require a careful interpretation of certain issues (Nicholls & Ward 2000; Ward *et al.* 2000). (1) Cationic lipophilic probes are nonselectively permeant across both plasma and mitochondrial membrane; (2) the distribution of the probe tends to a Nernst equilibrium across both membranes; (3) probe equilibrium is much faster across the small, highly invaginated inner mitochondrial membrane than across plasma membrane because of the much greater surface-to-volume ratio of the inner membrane–matrix compared with the

plasma membrane–cytoplasm. Typically, as we selected the best probe to use in our experiments, it is necessary to consider that this type of probes can be used in either quenching or non-quenching modes (Nicholls & Ward 2000; Duchen 2004). Quenching mode experiments require higher probe concentration (50-100 nM to several micromolar), which accumulates within mitochondrial matrix in a sufficient concentration to form aggregates, thus quenching some fluorescent emissions of the aggregated probe (a phenomenon called autoquenching) (Duchen 2004). Consequently, mitochondrial depolarization under these conditions will result in the release of the probe, un-quenching the loaded probe, and increasing the fluorescent signal in a transient manner. For this reason, and because quenching is a nonlinear event (Duchen 2004), quenching mode should only be used to monitor real-time effects on $\Delta\psi_m$ in response to acute application of an experimental treatment (i.e., pharmacologic or toxic treatments) during the imaging period (Nicholls & Ward 2000; Nicholls 2006; Ward *et al.* 2000). On the other hand, in non-quenching mode, lower probe concentrations are used (0.5-30 nM); thus, probe aggregation and quenching in the mitochondrial matrix does not occur. Experiments involving probe loading after experimental treatments affecting $\Delta\psi_m$ (i.e., chronic treatments done before probe loading to compare pre-existing relative mitochondrial polarization between control and experimental treatments), should typically utilize probes in non-quenching modes (Nicholls & Ward 2000; Nicholls 2006; Ward *et al.* 2000), since at very low concentrations, the fluorescent signal shows a linear relationship with the concentration of the probe. Thus, the concentration of the probe simply reflects the Nernstian distribution of the probe between compartments in response to local potential changes (Duchen 2004).

The empiric determination of the concentration of $TMRM^+$ in the mitochondrial matrix for our non-quenching experiments was the first step in our study. Figure 10 shows a representative gallery of fluorescent traces of purified nerve terminals equilibrated with different concentrations of $TMRM^+$ (100 nM, 50 nM, 25 nM, 15 nM, 10 nM and 7.5 nM) after addition of oligomycin/FCCP (black arrow). As observed for the higher concentrations of $TMRM^+$ (100-15 nM), when the purified nerve terminals are equilibrated

with sufficient probe to exceed the matrix quenching threshold, oligomycin/FCCP-induced mitochondrial depolarization caused a transient "spike" in whole purified nerve terminals $TMRM^+$ fluorescence, followed by a decay in the signal, due to loss of un-quenched component of the mitochondrial $TMRM^+$ fluorescence. These traces indicate that probe concentration in the matrix was sufficient to cause aggregation and quenching signal. On the other hand, when the loading corresponds to a subthreshold concentration (10 nM and 7.5 nM), there is only a decay of the signal, revealing that using these concentrations of $TMRM^+$ in nerve terminals allow us to work in a non-quenching mode.

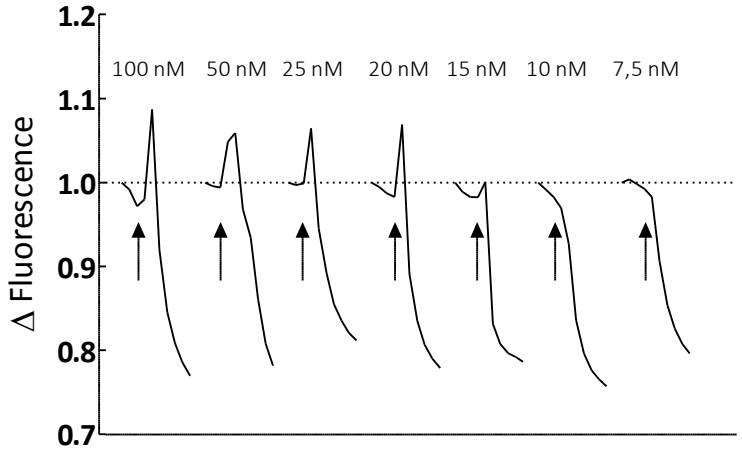

Figure 10: Quenching limit for $TMRM^+$ in the mitochondrial matrix. Plated purified nerve terminals were equilibrated in HBM medium supplemented with 1.2 mM $CaCl_2$ for 30 min with the indicated concentrations of $TMRM^+$. A cocktail of oligomycin (9 µg/mL) and FCCP (9 µM) was added to collapse $\Delta\psi_m$ when indicated by the arrow. The transient spike indicates a dequenching as the aggregated probe is released from the matrix.

4.2. Choice of an effective concentration of $A\beta_{1-42}$

Exposure of synaptosomes to $A\beta_{1-42}$ peptide has been reported to lead to the oxidative modification of proteins, supporting the role of $A\beta_{1-42}$ as an oxidative stress inducer (Boyd-Kimball *et al.* 2005). This protein oxidation can then lead to a variety of cellular consequences, namely mitochondrial dysfunction and ultimately to cell death (Poon *et al.* 2004). $A\beta_{1-42}$-induced mitochondrial dysfunction in synaptosomes was also described by Mattson and co-workers (Mattson *et al.* 1998b) and is considered a key feature in AD (Moreira *et al.* 2006). Indeed, soluble forms of β-amyloid, such as $A\beta_{1-42}$, have been described as a major malefactor in AD (Hardy & Selkoe 2002). Furthermore, decreased accumulation of $TMRM^+$ by $A\beta_{1-42}$-treated synaptosomes was also observed in fluorimetric assays, revealing decreased mitochondrial membrane potential (Canas *et al.* 2009).

We now evaluated the concentration of $A\beta_{1-42}$ required to observe alterations of mitochondrial properties in purified nerve terminals in the *in situ* functional experiments. Purified nerve terminals were incubated 2h with 50 nM or 500 nM of $A\beta_{1-42}$ following incubation with 7.5 nM of $TMRM^+$ for 30 minutes. Qualitative analyses of $\Delta\psi_m$ were done after live imaging experiments by calculating the difference between $TMRM^+$ fluorescence before and after addition of oligomycin and FCCP where we considered 100% the $\Delta\psi_m$ in control conditions and expressed the effect of $A\beta_{1-42}$ as a percentage change of $\Delta\psi_m$ compared to control. Figure 11 show that $\Delta\psi_m$ seems to be affected only in purified nerve terminals incubated with 500 nM of $A\beta_{1-42}$ peptide when compared with control situation. Analyses of the average $\Delta\psi_m$ in all types of purified nerve terminals shows that $A\beta_{1-42}$ caused a reduction of 24.0% ± 5.6% (n=9) of the $\Delta\psi_m$ compared with control.

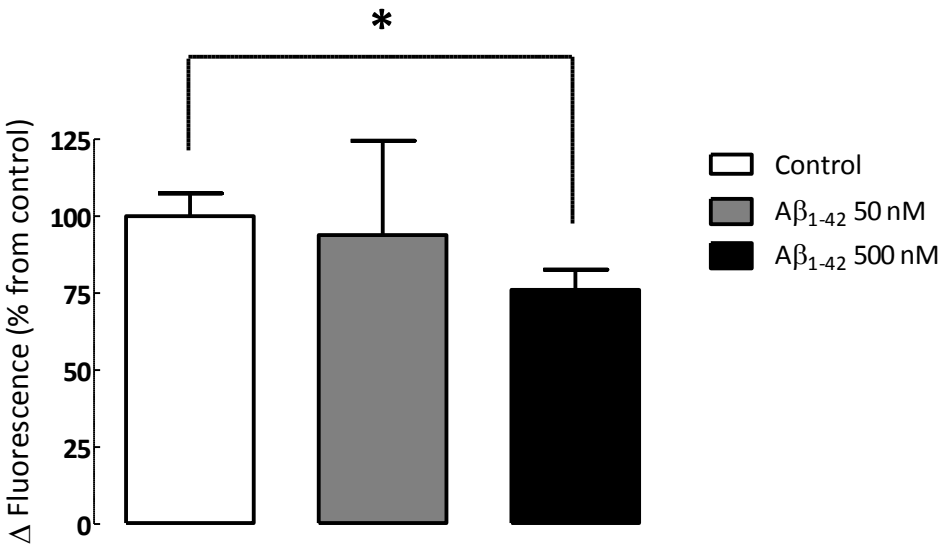

Figure 11: $\Delta\psi_m$ is affected in purified nerve terminals incubated with $A\beta_{1-42}$ peptide. Plated purified nerve terminals were incubated for 2 h with ultrapure water, 50 nM or 500 nM $A\beta_{1-42}$ in HBM medium supplemented with 1.2 mM $CaCl_2$ following 30 min of incubation with 7.5 nM $TMRM^+$. A cocktail of oligomycin (9 µg/mL) and FCCP (9 µM) were added to collapse $\Delta\psi_m$. The measurement of $\Delta\psi_m$ was done by calculating the difference between $TMRM^+$ fluorescence before and after addition of oligomycin and FCCP. We considered 100% the $\Delta\psi_m$ in control conditions and expressed the effect of $A\beta_{1-42}$ as a percentage change of $\Delta\psi_m$ compared to control. $^*P < 0.05$ compared to control using a paired Student's *t*-test analyses. Data are mean±SEM of n=9.

4.3. Measurement of mitochondrial membrane potential

In the present study an experimental protocol was devised to analyze qualitatively the $\Delta\psi_m$ status over a pathological condition from purified nerve terminals. Here, the effects of tested drugs were measured by calculating the difference between $TMRM^+$ fluorescence before and after addition of oligomycin and FCCP where we considered 100% the $\Delta\psi_m$ in control conditions and expressed the effect of $A\beta_{1-42}$ as a percentage change of $\Delta\psi_m$ compared to control.

As important controls depicted in figure 12, we first assessed the photobleaching of the probe (A and B). Also, the addition of the vehicle (EtOH) of the cocktail used as stimuli

was also tested to ensure that the effect seen on $\Delta\psi_m$ is due to the drugs rather than to the vehicle (C and D). Both measurements were done in the absence (control) and presence of $A\beta_{1\text{-}42}$.

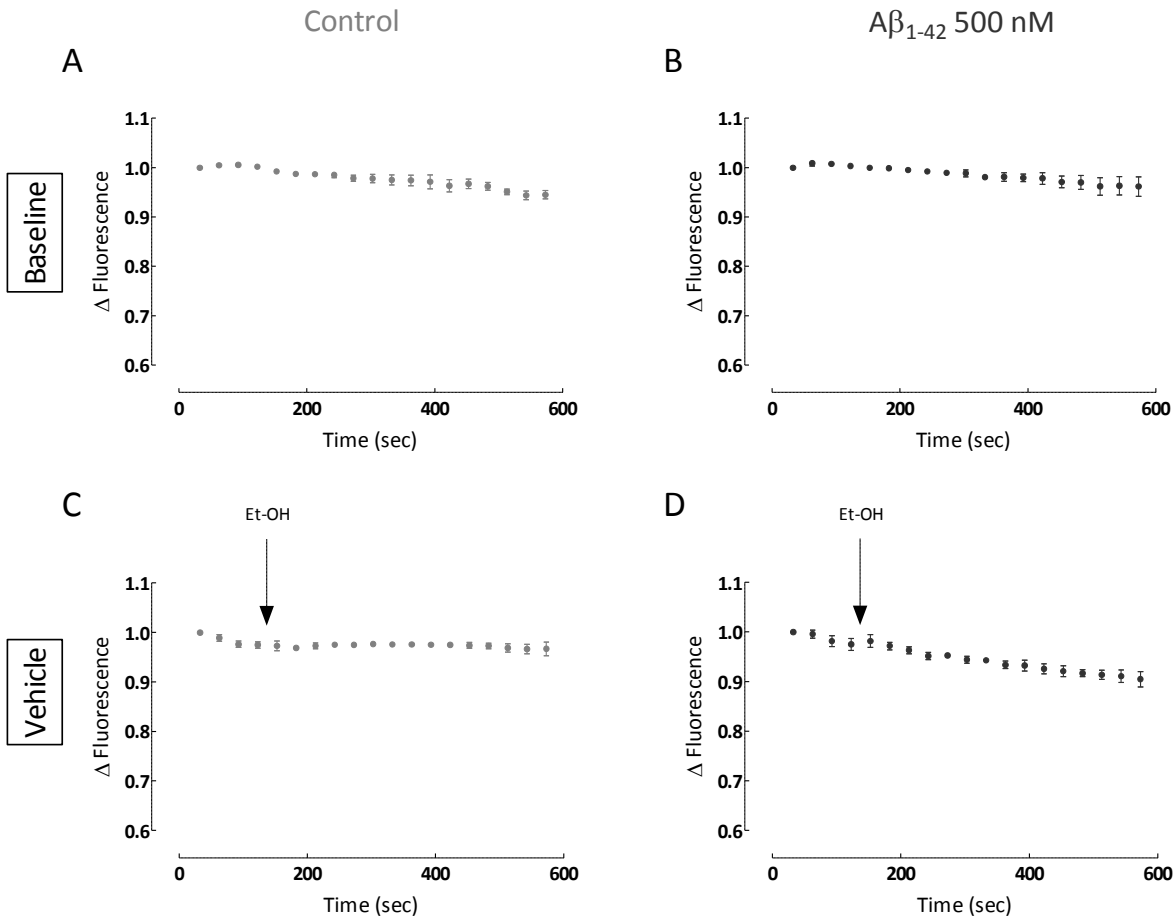

Figure 12: $\Delta\psi_m$ under experimental conditions. Plated purified nerve terminals were incubated for 2 h in the absence or presence of 500 nM $A\beta_{1\text{-}42}$ in HBM medium supplemented with 1.2 mM $CaCl_2$ following 30 min of incubation with 7.5 nM $TMRM^+$. The baseline of the probe was measured at every 30 second for a total of 10 minutes (A, B). The vehicle of the cocktail of oligomycin/FCCP was added at the 2.5 minutes and the fluorescence was measured for 10 min at every 30 second (C, D). The data are representative of n=3 for all conditions.

Figure 13A shows representative traces for the purified nerve terminals loaded with $TMRM^+$ after mitochondrial depolarization by addition of oligomycin/FCCP, which lead to a decay of $\Delta\psi_m$. The purified nerve terminals exposed to $A\beta_{1-42}$ present a lower extent of depolarization, as a consequence of a decrease accumulation of $TMRM^+$, which is indicative of defects on $\Delta\psi_m$. The analyses of the whole population of hippocampal nerve terminals show that $A\beta_{1-42}$ reduced the $\Delta\psi_m$ by 22.0% ± 5.1% (n=6) (Figure 12B).

A

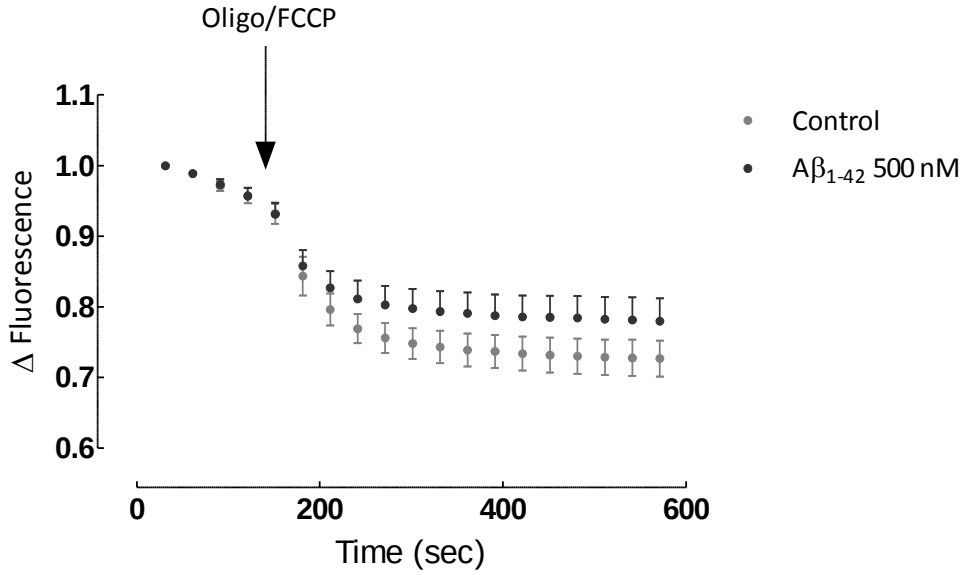

B

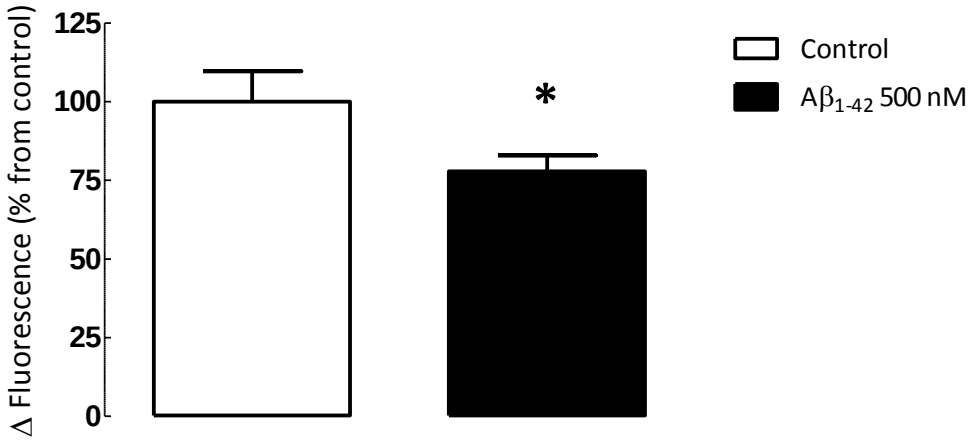

(Continues on next page)

Figure 13: $\Delta\psi_m$ is affected in whole population of hippocampal purified nerve terminals incubated with $A\beta_{1-42}$ peptide. (A) Plated purified nerve terminals on gridded coverslips were incubated for 2 h in the absence or presence of 500 nM $A\beta_{1-42}$ in HBM medium supplemented with 1.2 mM $CaCl_2$ following 30 min of incubation with 7.5 nM $TMRM^+$. A cocktail of oligomycin (9 µg/mL) and FCCP (9 µM) was added at 2.5 minutes to collapse $\Delta\psi_m$ following an establishment of a new baseline. The fluorescence of the probe was measured at every 30 second for a total of 10 minutes. The data are representative of n=6 for both conditions. (B) Representation of the measurement of $\Delta\psi_m$ calculated through the difference between $TMRM^+$ fluorescence before and after addition of oligomycin and FCCP. We considered 100% the $\Delta\psi_m$ in control conditions and expressed the effect of $A\beta_{1-42}$ as a percentage change of $\Delta\psi_m$ compared to control. The results represent a paired Student's *t*-test analyses comparing with the hypothetical value of 100, presenting a reduction of reduction of 22.0% ± 5.1% (mean±SEM of n=6, $*P < 0.05$).

4.4. Immunocytochemistry:

To investigate presynaptic mitochondria in glutamatergic nerve terminals we used a double immunocytochemistry strategy consisting on the simultaneous labeling of a selective marker of glutamatergic nerve terminals and a marker of the mitochondrial outer-membrane protein. Purified nerve terminals, plated in gridded coverslips, were subject to immunocytochemistry after the *in situ* experiments for a final assessment of the changes of $\Delta\psi_m$ in glutamatergic nerve terminals. In parallel, labeling of the mitochondrial outer-membrane allowed the identification of mitochondria in nerve terminals.

For this purpose, we were used antibodies against: i) the vesicular glutamate transporter 1 (VGLUT1), one type of vesicular neurotransmitter transporters (VNTs), and a specific protein marker of neurons that use glutamate as neurotransmitter, and ii) the mitochondrial preprotein translocases of the outer membrane (Tom20). Vesicular glutamate transporters (VGLUTs) can be classified at least in three different subtypes (VGLUT1-3) (Wojcik *et al.* 2004). VGLUT1 and VGLUT2 display roughly complementary expression patterns in the CNS with only a limited overlap (Fremeau *et al.* 2001; Fujiyama *et al.* 2001; Herzog *et al.* 2001; Kaneko & Fujiyama 2002). VGLUT1 is mainly present in the cortex, hippocampus and amygdala (Fremeau *et al.* 2001; Hisano *et al.* 2002; Liguz-Lecznar

& Skangiel-Kramska 2007). VGLUT2 is present in olfactory bulb, cortex dentate gyrus of hippocampus, thalamus, hypothalamus and brain stem (Fremeau *et al.* 2001; Fujiyama *et al.* 2001; Herzog *et al.* 2001; Kaneko & Fujiyama 2002). On the other hand, VGLUT3 is localized in a limited number of glutamatergic neurons in several regions, such as the neocortex, hippocampus, olfactory bulb, hypothalamus, substantia nigra, and raphe nuclei (Fremeau *et al.* 2002; Gras *et al.* 2002; Schäfer *et al.* 2002; Herzog *et al.* 2004). Additionally, VGLUT3 is also present in a population of symmetrical synapses, such as in hippocampal and cortical GABAergic neurons (Herzog *et al.* 2004), striatal cholinergic neurons and in serotonergic neurons in raphe nuclei (Herzog *et al.* 2004; Schäfer *et al.* 2002). Thus, the identification of glutamatergic neurons has mainly relied on VGLUT1 marker, since VGLUT3 can also be localized in non-glutamatergic neurons, such as, in some GABAergic and cholinergic neurons.

Although the relative densities of glutamatergic nerve terminals in the hippocampus have already been determined (Köfalvi *et al.* 2005; Rebola *et al.* 2005), we first quantified the number of platted purified nerve terminals that are VGLUT1-immunopositive and that co-localized with Tom20-immunopositive nerve terminals (Figure 14). The immunochemical quantification showed no difference of the relative number of glutamatergic nerve terminals between the $A\beta_{1-42}$-treated purified nerve terminals when compared to the control. However, it is noticed that the $A\beta_{1-42}$-treated purified nerve terminals seems to have a tendency to have decreased percentage of glutamatergic nerve terminals. This was expected since we carried out an acute treatment of the purified nerve terminals with $A\beta_{1-42}$ and it takes several days after exposure to $A\beta_{1-42}$ to reveal a decrease of the density of glutamatergic nerve terminals in the hippocampus (Canas *et al.* 2014).

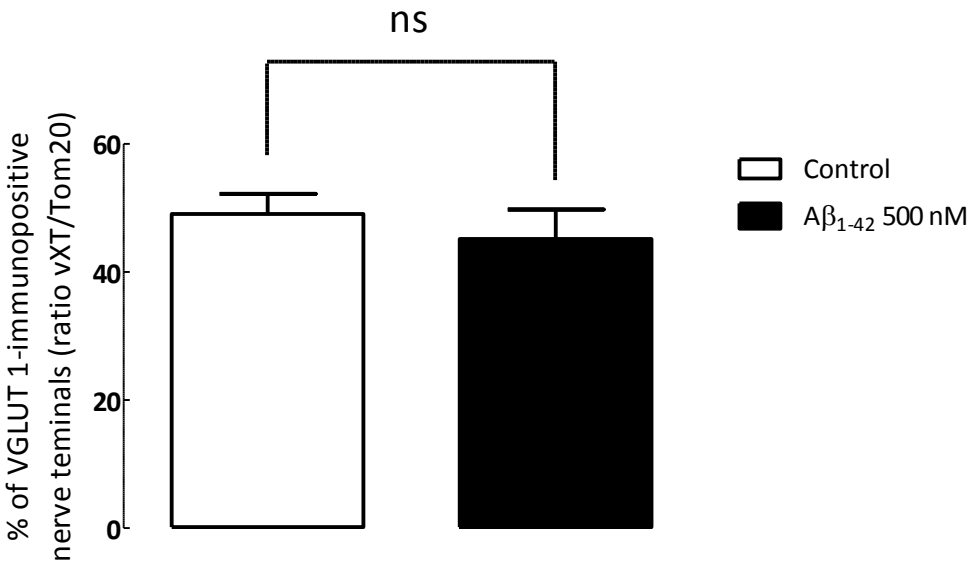

Figure 14: Immunochemical quantification of hippocampal purified nerve terminals immunopositive for VGLUT1 and Tom20, in control conditions (water) and after incubation with 500 nM $A\beta_{1-42}$ peptide. Representation of the percentage of VGLUT1-immunopositive purified nerve terminals in relation to Tom20-immunopositive elements. The results are presented as mean±SEM of n=6 independent experiments. ns – non significant ($P > 0.05$).

Through this immunocytochemistry approach, we were able to identify which purified nerve terminals analyzed through *in situ* experiments correspond to glutamatergic nerve terminals. Thus, we specifically analyzed the changes of the $\Delta\psi_m$ upon exposure to $A\beta_{1-42}$ in glutamatergic nerve terminals. We observed a reduction of 23.0% ± 5.2% (n=6) of $\Delta\psi_m$ in the VGLUT1-immunopositive nerve terminals treated with $A\beta_{1-42}$ compared with control (Figure 15A and 15B).

A

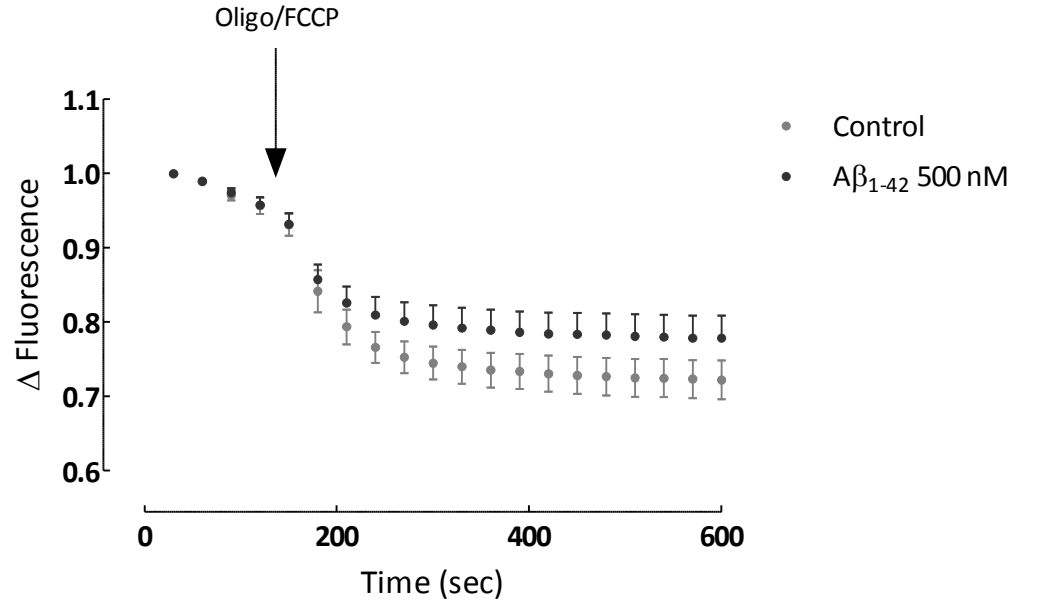

B

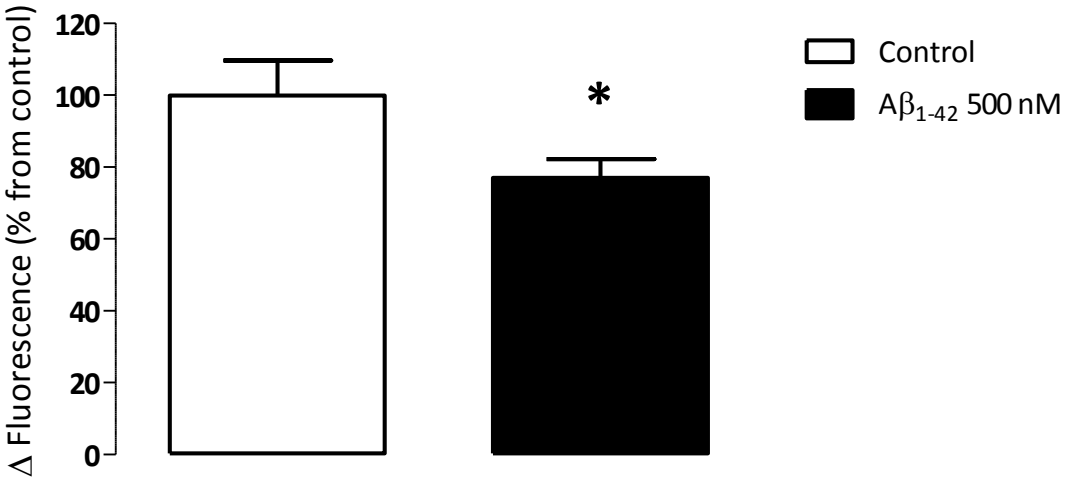

(Continues on next page)

C

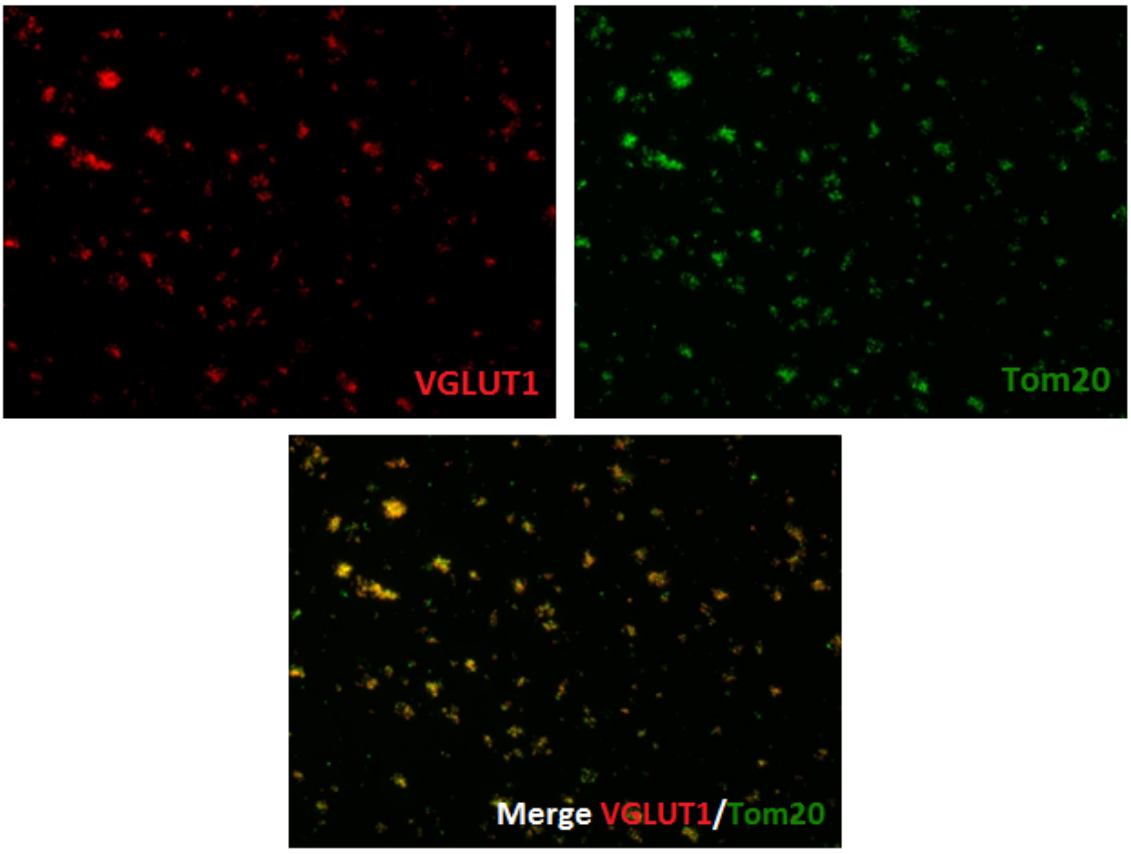

Figure 15: Reduction of *in situ* $\Delta\psi_m$ from glutamatergic nerve terminals caused by $A\beta_{1\text{-}42}$ peptide. (A) Plated purified nerve terminals on gridded coverslips were incubated for 2 h in the absence or presence of 500 nM $A\beta_{1\text{-}42}$ in HBM medium supplemented with 1.2 mM $CaCl_2$ following 30 min of incubation with 7.5 nM $TMRM^+$. A cocktail of oligomycin (9 µg/mL) and FCCP (9 µM) was added at 2.5 minutes to collapse $\Delta\psi_m$ following an establishment of a new baseline. The fluorescence of the probe was measured at every 30 second for a total of 10 minutes. The data are representative of n=6 for both conditions from VGLUT1-immunopositive nerve terminals. (B) Representation of the measurement of $\Delta\psi_m$ calculated through the difference between $TMRM^+$ fluorescence before and after addition of oligomycin and FCCP from VGLUT1-immunopositive nerve terminals. We considered 100% the $\Delta\psi_m$ in control conditions and expressed the effect of $A\beta_{1\text{-}42}$ as a percentage change of $\Delta\psi_m$ compared to control. The results represent a paired Student's *t*-test analyses comparing with the hypothetical value of 100, presenting a reduction of reduction of 23.0% ± 5.2% (mean±SEM of n=6, $^*P < 0.05$). (C) Representative image of the images taken from VGLUT1 (Alexa

Flour 594, red) and Tom20 (Alexa Flour 647, green) immunolabbeling, and the merge images that represent the colocalization between VGLUT1 and Tom20 labeling (yellow). The magnification used to obtain the images was 63×.

Notably, it seems that $A\beta_{1-42}$ specifically affected $\Delta\psi_m$ in glutamatergic nerve terminals. In fact, the analysis of non-glutamatergic nerve terminal showed that, after addiction of oligomycin/FCCP no difference is observed in $\Delta\psi_m$ comparing $A\beta_{1-42}$-treated purified nerve terminals with control nerve terminals (Figure 16).

A

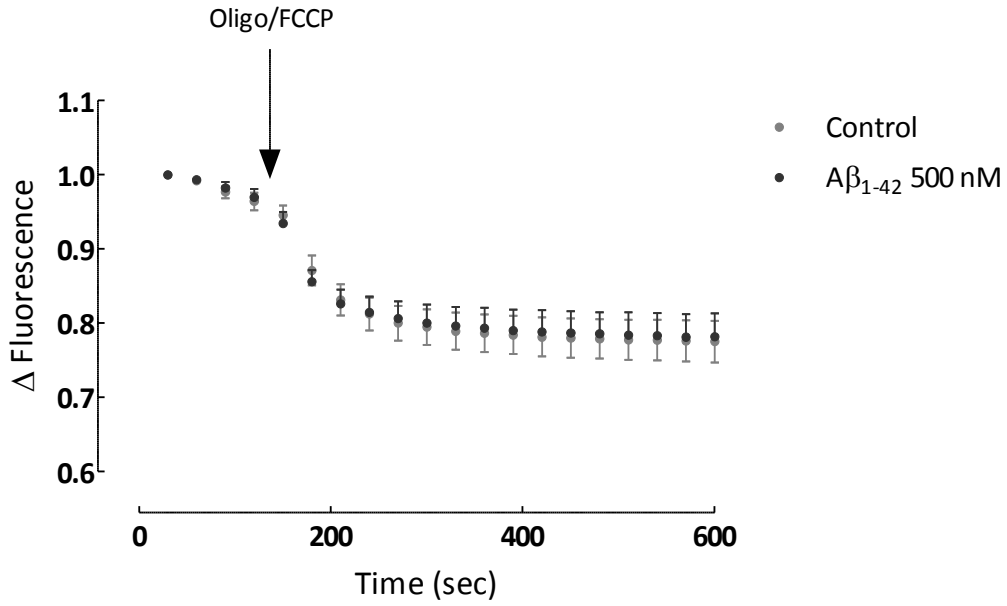

(Continues on next page)

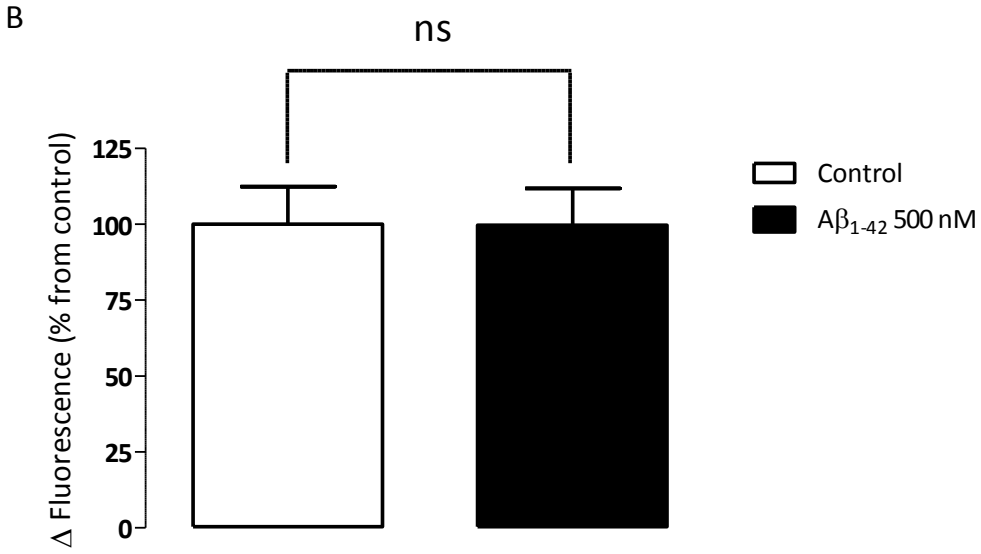

Figure 16: $\Delta\psi_m$ is not affected in non-glutamatergic nerve terminals. (A) Plated purified nerve terminals on gridded coverslips were incubated for 2 h in the absence or presence of 500 nM $A\beta_{1-42}$ in HBM medium supplemented with 1.2 mM $CaCl_2$ following 30 min of incubation with 7.5 nM $TMRM^+$. A cocktail of oligomycin (9 µg/mL) and FCCP (9 µM) were added at 2.5 minutes to collapse $\Delta\psi_m$ following an establishment of a new baseline. The fluorescence of the probe was measured at every 30 second for a total of 10 minutes. The data are representative of n=6 for both conditions from nerve terminals that were not VGLUT1-immunopositive. (B) Representation of the measurement of $\Delta\psi_m$ calculated through the difference between $TMRM^+$ fluorescence before and after addition of oligomycin and FCCP from purified nerve terminals that were not VGLUT1-immunopositive. We considered 100% the $\Delta\psi_m$ in control conditions and expressed the effect of $A\beta_{1-42}$ as a percentage change of $\Delta\psi_m$ compared to control. The results represent a paired Student's *t*-test analysis comparing with the hypothetical value of 100. The results are presented as mean±SEM of n=6 independent experiments. ns – non significant ($P > 0.05$).

4.5. Assessment of alterations of the plasma membrane potential

The use of cationic, cell permeant, fluorescent probes as $\Delta\psi_m$ indicators requires an additional and imperative control: to ensure that any observed changes in fluorescence are indeed due to changes in $\Delta\psi_m$ rather than in $\Delta\psi_p$. Such controls is of uppermost important since the uptake and equilibrium of these types of probes within the mitochondrial matrix in cells has as equal contribution of both $\Delta\psi_p$ and $\Delta\psi_m$ (Nicholls 2006).

To resolve this question, anionic membrane-permeant probes can be used. Because of their negative charge, these types of probes are excluded from polarized cells due to the negative membrane potential, entering the cells only under plasma membrane depolarization. Thus, mitochondria and their negative membrane potential do not accumulate these types of probes. An appropriate plasma membrane potential kit assay (Molecular Devices, Sunnyvale, USA) has become available (Baxter *et al.* 2002). Here, we have used the fluorescent anion (named PMPI) to assess eventual changes on $\Delta\psi_p$ using wavelength (nm) of excitation and the emission of this probe similar to these used for $TMRM^+$.

We again carried out experiments depicted in figure 17, where the photobleaching of the probe was tested (A and B), as well as the impact of the addition of the vehicle (EtOH) of the cocktail used as stimuli was also tested (C and D). Both measurements were done in the absence (control) and in the presence of 500 nM $A\beta_{1-42}$. From the upper panel of figure 17 we can see that incubation of purified nerve terminals with $A\beta_{1-42}$ *per se* does not cause depolarization of nerve terminals (17B).

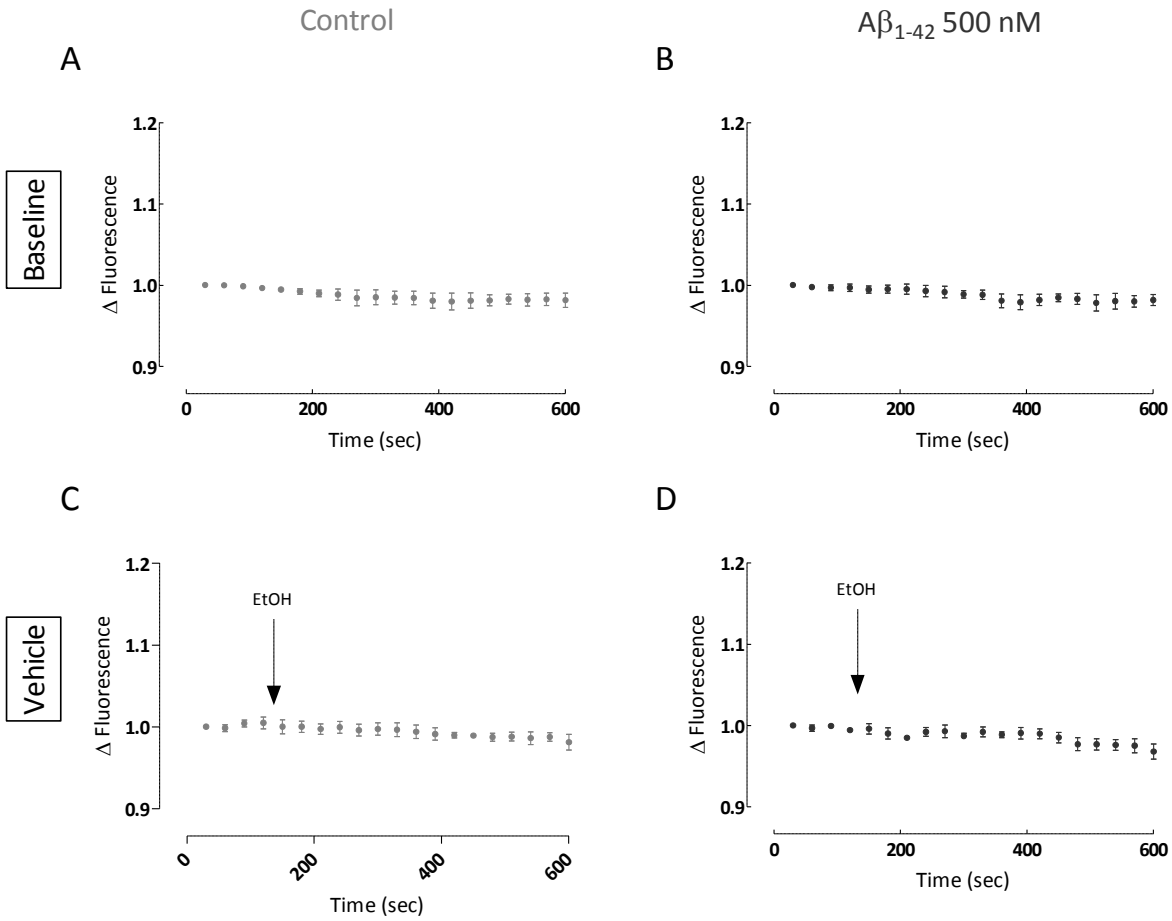

Figure 17: $\Delta\psi_p$ under experimental conditions. Plated purified nerve terminals were incubated for 2 h in the absence or presence of 500 nM $A\beta_{1-42}$ in HBM medium supplemented with 1.2 mM $CaCl_2$ following 30 min of incubation with PMPI (1 µL/mL). The baseline of the probe was measured at every 30 seconds for a total of 10 minutes (A, B). The vehicle of the cocktail of oligomycin (9 µg/mL) and FCCP (9 µM) was added at the 2.5 minutes and the fluorescence was measured for 10 min at every 30 seconds (C, D). The data are representative of n=3 for all conditions.

Although the use of PMPI has already been validated in cultured neurons (Nicholls 2006), as far as we know, its use in purified nerve terminals was never tested before. So, before testing if oligomycin/FCCP affected the $\Delta\psi_p$, we assessed if a variation on $\Delta\psi_p$ is accompanied by changes on PMPI fluorescence.

Figure 18 shows a representative traces for the purified nerve terminals loaded with PMPI after plasma membrane depolarization by addition of 30 mM KCl, as previous reported (Tretter *et al.* 1998). A fast increase in fluorescence was observed followed by a decay of fluorescence. With this data, we prove that PMPI can indeed be used in purified nerve terminals, which enabled us to probe if fluctuations of $\Delta\psi_p$ contributed for our purportedly measured $\Delta\psi_m$.

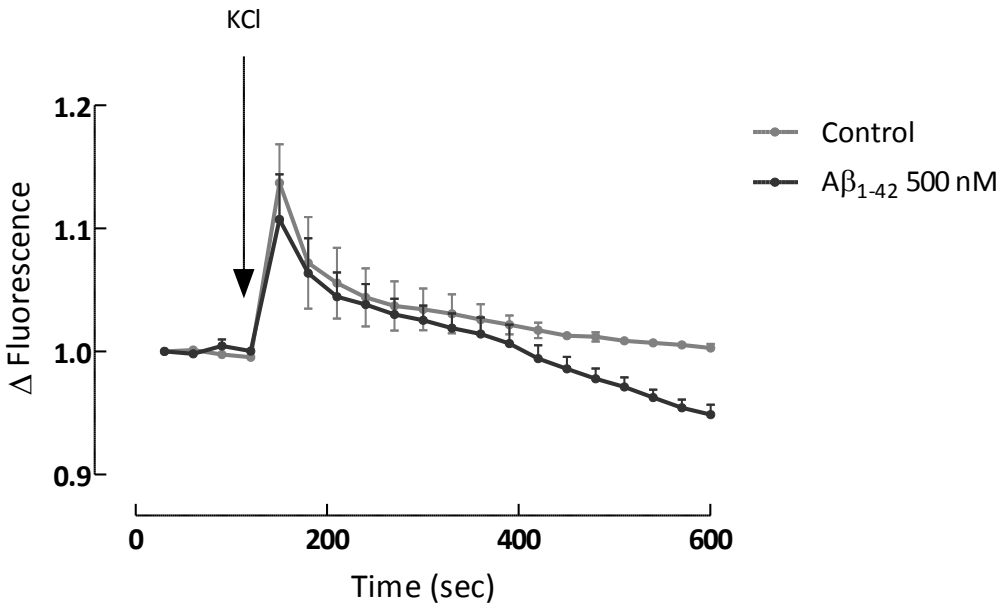

Figure 18: PMPI validation in purified nerve terminals. Plated purified nerve terminals were loaded with PMPI (1 µL/mL) for 30 minutes. The addition of 30 mM KCl caused an initial increase of fluorescence emission (i.e. $\Delta\psi_p$, a depolarization) in both control nerve terminals and in nerve terminals exposed to 500 nM $A\beta_{1-42}$. After a transient increase of the fluorescence we observed the repolarization of the nerve terminals, as concluded from the rapid decay of emitted fluorescence. The data are representative of n=3 for both conditions.

Besides being widely used to depolarize mitochondria, is known that protonophores, such as FCCP, can also affect $\Delta\psi_p$ at higher concentrations (Rottenberg & Wu 1998). Thus, after the validation of the use of PMPI on purified nerve terminals, we went asses if the

addition of oligomycin/FCCP, represent changes on $\Delta\psi_p$ in addition to observed changes in $\Delta\psi_m$.

Addiction of oligomycin/FCCP to purified nerve terminals previously loaded with PMPI did not modify the measured $\Delta\psi_p$ (Figure 19). This further confirms that the PMPI signal truly reflects changes in $\Delta\psi_p$, and also ensures the validity of our $\Delta\psi_m$ experiments.

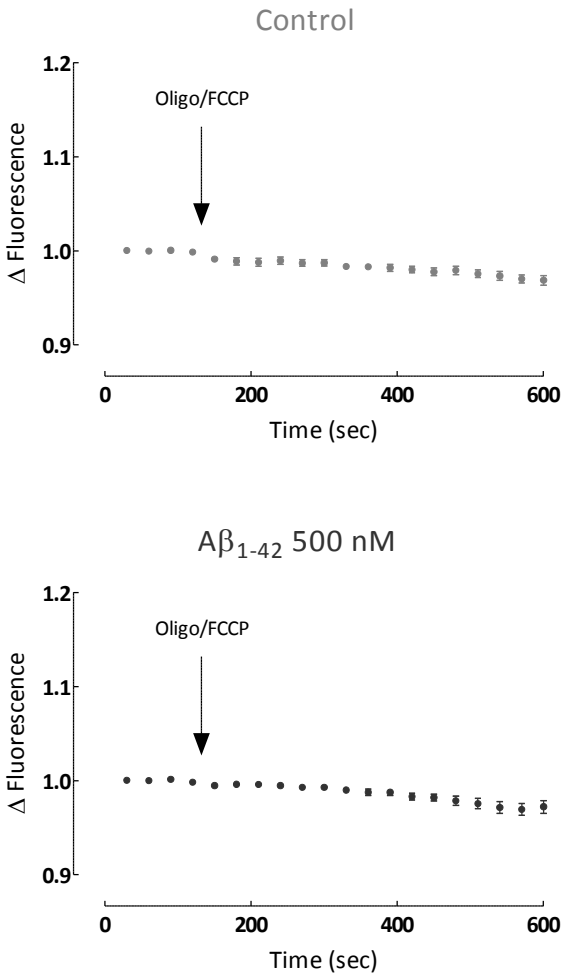

Figure 19: $\Delta\psi_p$ monitoring removes ambiguity from $\Delta\psi_m$. Plated purified nerve terminals incubated for 2 h in the absence or presence of 500 nM $A\beta_{1-42}$ in HBM medium supplemented with 1.2 mM $CaCl_2$ following 30 min of incubation with PMPI (1 µL/mL). A cocktail of oligomycin (9 µg/mL) and FCCP (9 µM) were added at 2.5 minutes to evaluate de contribution of $\Delta\psi_p$ on $\Delta\psi_m$ measurements. No effect on $\Delta\psi_p$ was observed after administration of oligomycin/FCCP. The fluorescence of the probe was measured at every 30 seconds for a total of 10 minutes. The data are representative of n=4 for both conditions.

Finally, one of our major concerns was to have a maximum control of the experiences. Thus we also assessed the effect of the addition of 30 mM KCl on purified nerve terminals loaded with $TMRM^+$. We observed that 30 mM KCl caused a decay of the $\Delta\psi_m$ (Figure 20). Comparing figures 13A and 15A with figure 20, it seems that the decay of the $TMRM^+$ fluorescence is faster after adding oligomycin/FCCP than after adding KCl.

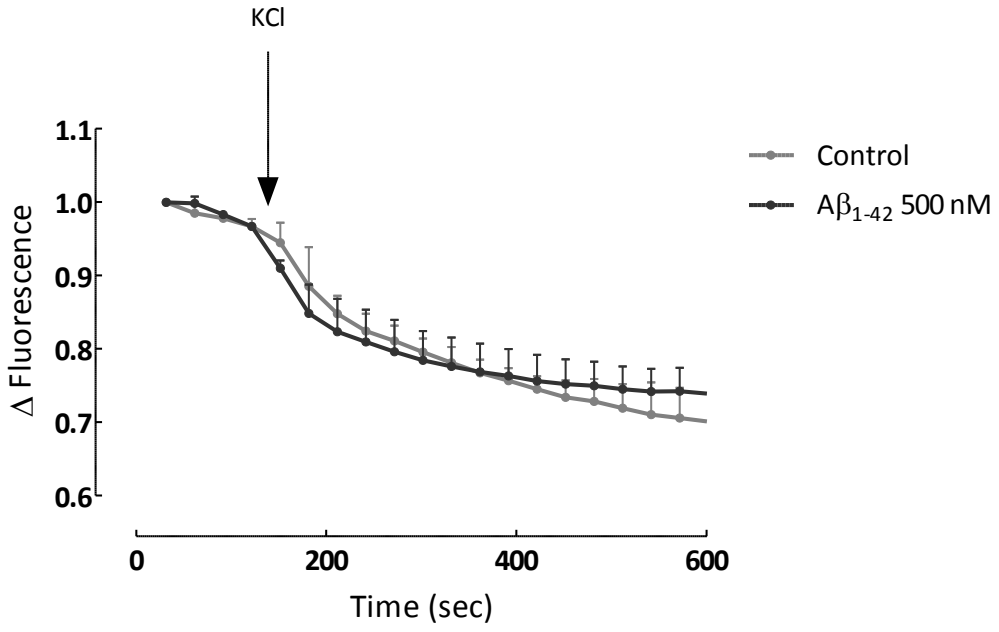

Figure 20: $\Delta\psi_m$ depolarization by KCl. Purified nerve terminals were incubated for 2 h in the absence or presence of 500 nM $A\beta_{1\text{-}42}$ in HBM medium supplemented with 1.2 mM $CaCl_2$ following 30 min of incubation with 7.5 nM $TMRM^+$. A 30 mM KCl added at 2.5 minutes to collapse $\Delta\psi_m$ following an establishment of a new baseline. The fluorescence of the probe was measured at every 30 seconds for a total of 10 minutes. The data are representative of n=3 for both conditions.

5. DISCUSSION

An important goal of our work was to develop appropriate techniques to properly assess the bioenergetic status of mitochondria specifically in glutamatergic nerve terminals. By combining *in situ* experiments with double immunocytochemistry assays in single nerve terminals we could assess particular alterations on mitochondria bioenergetic status in an Aβ-based model of AD. Nerve terminals, due their unique high energy demands, are particularly sensitive to bioenergetic defects (Choi *et al.* 2012). Thus, potential impacts on synaptic mitochondrial dysfunction may be a causative factor leading to synaptic loss, a hallmark of early AD, which might become an attractive hypothesis to understand the development of AD (Choi *et al.* 2012).

However, monitoring changes in *in situ* $\Delta\psi_m$ needs a careful experimental interpretation, since membrane-permeant cations can accumulate across the plasma and the mitochondrial membranes and $\Delta\psi_m$ can be critically contaminate by $\Delta\psi_p$. Quenching and non-quenching modes, the two modes employed for fluorescent cationic indicators, were carefully distinguished due their opposite responses to changes in $\Delta\psi_m$. We could observe, as previous described (Nicholls 2006), that in a quenching mode using an high probe concentration, aggregation and quenching occurs in the matrix; under such conditions, mitochondrial depolarization results in an increase in whole nerve terminals fluorescence as the probe is released into the cytoplasm. This increase is however transient because the excess of cytoplasmic probe redistributes across the plasma membrane in order to restore the Nernst equilibrium. For this reason, the quench mode is favored for studies using probes such as rhodamine 123, which are relatively slowly permeant across the plasma membrane. However, due to its low permeability, the quantification of rhodamine becomes difficult, since rhodamine is usually loaded by brief exposure to very high concentration of the probe (i.e. micromolar) (Keelan *et al.* 1999). The non-quenching mode, on the other hand, can follow slow changes in $\Delta\psi_m$, allowing distinguishing between nerve terminals containing mitochondria with different steady-state potentials.

In this study, we demonstrate that the exposure of nerve terminals to $A\beta_{1-42}$ peptides triggers defects in the $\Delta\psi_m$. This finding is in agreement with data previously reported by

our group (Canas *et al.* 2009). However, the previous work was performed in whole synaptosomal populations. We now aimed to analyze changes in the $\Delta\psi_m$ in purified nerve terminals (i.e., only in the presynaptic component of the synapse) and specifically in glutamatergic nerve terminals, the type of nerve terminals that are initially affected in an Aβ-based model of AD (Canas *et al.* 2014).

Importantly, some studies have verified the quality of the nerve terminals since their obtention involves several putatively disruptive steps (Joyce *et al.* 2003; Choi *et al.* 2012). Additionally, Paula Canas and colleagues (Canas *et al.* 2009) have demonstrated that synaptosomes exposed to $A\beta_{1-42}$ peptide for 2h are capable of maintaining their viability. However, in our study, we only assess the $\Delta\psi_m$ from glutamatergic nerve terminals that were functional in the *in situ* experiments, in other words, those nerve terminals loaded with $TMRM^+$ that responded to mitochondria depolarization after stimuli with oligomycin and FCCP. Indeed, using an immunochemical approach we were able to selectively analyze the nerve terminals immunopositive for VGLUT1 and Tom20, corresponding to glutamatergic nerve terminals containing mitochondria. We observed that the percentage of glutamatergic nerve terminals in the hippocampus was similar to that described previously (Canas *et al.* 2014). As expected, we did not observe a modification of the number of glutamatergic nerve terminals upon $A\beta_{1-42}$-treatment, since we carried out an acute exposure and it takes several days to observe the selective loss of glutamatergic terminals after the exposure to $A\beta_{1-42}$ (Canas *et al.* 2014). Additionally, the Aβ-based model of AD used in our work was different from the one previously used. Here we used an *in vitro* Aβ-based model where we incubate plated nerve terminals with $A\beta_{1-42}$ peptide, contrary to the *in vivo* Aβ-based model where $A\beta_{1-42}$ peptide fragment was administered intracerebroventricularly.

The most striking finding revealed by our immunocytochemistry assays was that glutamatergic nerve terminals displayed a reduction in the $\Delta\psi_m$ upon exposure to $A\beta_{1-42}$, whereas non-glutamatergic nerve terminals did not display such an $A\beta_{1-42}$-induced decrease of the $\Delta\psi_m$. This indicates the involvement of presynaptic mitochondria on the glutamatergic dysfunction in early AD.

These data prompt the hypothesis that presynaptic mitochondria within glutamatergic synapses may be responsible for the susceptibility of glutamatergic nerve terminals triggering dysfunction and damage in this animal model of AD. This main conclusion give us new information about the particular vulnerability of the glutamatergic nerve terminals in early AD, since the identification was based on VGLUT1, a reliable glutamatergic terminal marker (Takamori *et al.* 2000), and where presynaptic mitochondria is compromised. These results are in agreement with previous reports describing a toxicity of Aβ oligomers to synaptosomal mitochondria (Keller *et al.* 1997; Guo *et al.* 2000). Additionally, Begley and colleagues (Begley *et al.* 1999) using a transgenic AD-related synaptosomal model, have reported defects on $\Delta\psi_m$. Moreover, these results are also supported by data described by Du and co-workers (Du *et al.* 2010), where they show that synaptic mitochondria are more susceptible to Aβ-induced damage highlighting mitochondrial dysfunction. They have shown that a progressively accumulation with age of $A\beta_{1\text{-}42}$ in Tg mAPP synaptic mitochondria is responsible for the decline of both respiratory function and cytochrome c oxidase activity as well as the increase in mitochondrial oxidative stress. They also observed that this Aβ accumulation occurs before extensive extracellular Aβ deposits according with previous reports showing that intracellular and mitochondrial accumulation of Aβ occur before extracellular Aβ deposits (Caspersen *et al.* 2005). Furthermore, Brian Billups and Ian Forsythe (Billups & Forsythe 2002) have reported that mitochondria are a major organelle regulating presynaptic Ca^{2+} levels at the central glutamatergic system, a regulation which is highly dependent on $\Delta\psi_m$ (Duchen 2004; Rizzuto *et al.* 2004). Nevertheless, some groups of investigators have reported data which do not support the data presented here. Sung Choi and colleagues (Choi *et al.* 2012) in a different animal model of AD have reported that presynaptic nerve terminals from the hippocampus maintained their intrinsic bioenergetic capacities. Additionally, Karen Bell and Claudio Cuello (Bell & Cuello 2006) using another different animal models have observed that the cholinergic terminals appears the most vulnerable followed by the glutamatergic and GABAergic nerve terminals. These different reports regarding the affection of nerve terminals in early AD may be explained due to

different metabolic demands in glutamatergic nerve terminals versus non-glutamatergic nerve terminals (Wurtman 1992). Moreover, since the percentage of cholinergic nerve terminals in the hippocampus represent approximately 5% of the total nerve terminals (Degroot *et al.* 2006) during our experiments we may lose the viability of almost all these nerve terminals or they could not have functional mitochondria. Additionally, mitochondrial density may vary between glutamatergic versus non-glutamatergic nerve terminals. One of the amazing proprieties of synapses it is their ability to transmit a variety of messages adjusting their strength presynaptically by changing the amount of neurotransmitters released is response a given signal (O'Connor *et al.* 2005). Apart from causing structural changes in the presynaptic compartment, CNS synapses also show a considerable variation in their presynaptic mitochondria content (Shepherd & Harris 1998). Although, despite the fact that mitochondria are part of the presynaptic structure, not all the synapses have mitochondria (Shepherd & Harris 1998; Waters & Smith 2003). It has been suggested that those mitochondria-free presynaptic terminals are inactive or temporarily without mitochondria, once mitochondria can relocate into and out synapses depending on its activity (Rintoul *et al.* 2003; Kang *et al.* 2008). Thus, sites with highly energy demands, such as active synapses (Hollenbeck & Saxton 2005), increasing energy demands (e.g. increased ADP/ATP ratio) could facilitate the recruitment of mitochondria to synapses (Mironov 2007).

As already mentioned, Aβ can be located to synaptic mitochondria. Thus, over the years, several studies investigated the mechanisms of mitochondrial Aβ uptake. First, Devi and co-workers (2006) found abnormal Aβ accumulation across mitochondrial important channels, which lead to mitochondrial dysfunction (Devi *et al.* 2006). Two years later Camilla Hansson Petersen and colleagues (Hansson Petersen *et al.* 2008) reported that Aβ peptide is imported into mitochondria via the TOM complex machinery, when applied both extracellularly or directly to isolated mitochondria. Additionally, they have shown that, Aβ do not block the outer membrane import pore. However, Sirk and colleagues (Sirk *et al.* 2007), showed that upon chronic exposure, Aβ inhibits mitochondrial import of nuclear-encoded proteins, suggesting that chronic exposure to Aβ could indeed contribute

to mitochondria impairment on AD. Camilla Hansson Petersen and colleagues (Hansson Petersen *et al.* 2008) also suggested that, after import, Aβ is inserted into the inner mitochondria membrane and that only a small portion of the Aβ is loosely attached. These results correlate with results showing that $A\beta_{1-42}$ may cause inhibition of ETC complex I and IV (Bobba *et al.* 2013; Crouch *et al.* 2005). Our results appear be in line with these previous reports since reduced ETC efficiency due Aβ binding will disturb the generation of a proton motive force and consequently will affect $\Delta\psi_m$ which in turn is required for the import of matrix proteins (Neupert & Herrmann 2007) essential for mitochondrial biogenesis.

Several lines of evidence have suggested that steady-state levels of Aβ are dependent of the balance between Aβ generation and clearance in which the disruption of this clearance gives rise to increased Aβ accumulation. Regarding this, Nyosha Alikhani and colleagues (Alikhani *et al.* 2011) have found that presequence peptidase, a novel mitochondrial Aβ-degrading enzyme present in the matrix, named PreP peptidasome (Falkevall *et al.* 2006), has a lower proteolysis activity as a consequence of ROS production, contributing to Aβ accumulation in AD brain mitochondria. Additionally, it was described that both the inhibition of ETC complexes, which increases the production of mitochondrial ROS, and the impairment of energy production, will elevate β-secretase activity facilitating the cleavage of APP (Hemachandra & Flint 2008; Velliquette *et al.* 2005). Here, we postulate that Aβ may be responsible for synaptic mitochondria dysfunction in early AD, which will start a cascade of events leading to synapse loss. In the early-onset of the disease, Aβ may trigger synaptic mitochondria, and among others, may increase ROS production, decrease of $\Delta\psi_m$ and decrease ATP production which consequently, will lead to impaired bioenergetics impairing neuronal function and exacerbating neurodegeneration. During the development of AD, this continuous increase of ROS production will then elevate β-secretase activity, facilitating the cleavage of Aβ leading to mitochondrial and intracellular deposits before extracellular deposits.

Finally, regarding our PMPI experiments, it is described that, in *in situ* experiments where low probe concentrations are used in order to evaluate pre-existing values of $\Delta\psi_m$,

a great precaution has to be taken into account since observed changes in fluorescence can be due changes in $\Delta\psi_m$, $\Delta\psi_p$, or both (Nicholls 2006). However, we were faced with an issue since the use of the probe PMPI as far as we know never was tested in purified nerve terminals. With the most popular strategy to depolarize synaptosomes (Scott & Nicholls 1980), KCl-induced plasma membrane depolarization show, for the first time and as far as we know, that the probe PMPI can indeed be used to measure or access $\Delta\psi_p$ in purified nerve terminals. We could also observe that, after plasma membrane depolarization, $A\beta_{1-42}$-incubated purified nerve terminals fail to retain the probe which appears be in line with previous reports showing that Aβ induce lipid peroxidation in synaptosomes after 1h of exposure (Keller *et al.* 1997).

Simultaneous monitoring of changes in $\Delta\psi_m$ and $\Delta\psi_p$ with dual labeling with $TMRM^+$ and PMPI would be a better choice for these experiments, however, due to limitations in our equipment's and because the spectra of both probes are very similar, we had to measure both potentials separately. In our experiments we observe that the addition of oligomycin/FCCP did not effects $\Delta\psi_p$. This contrast with previous studies reporting that significant changes in $\Delta\psi_p$ occur with the use of FCCP and oligomycin at low micromolar concentration (Nicholls 2006). On the other and, Daniel Farkas and colleagues (Farkas *et al.* 1989) several years ago have reported that using a wide range of FCCP concentrations (0.1-10 μM) couldn't find any qualitative distinction in plasma membrane fluorescence of cells loaded with TMRE, only a small depolarization that they argue be due plasma membrane depolarization by FCCP or due to ATP depletion from cells. In our experiments we have used higher concentrations of both oligomycin and FCCP. This is explained due to the fact that we pretended to determine the mitochondrial accumulation of $TMRM^+$ under physiological and pathological conditions and, to do that, we needed to use higher concentrations of both oligomycin and FCCP, as previous reported (Joyce *et al.* 2003), to make sure that we reach zero $\Delta\psi_m$ since mitochondrial depolarization, with decrease of $\Delta\psi_m$, does not indicate necessarily mitochondrial respiratory chain dysfunction (Oliveira 2012). As previous reported the addiction of 5 μL of oligomycin/FCCP to the 500 μL of medium in the perfusion chamber decreased $\Delta\psi_m$ and had no effect on $\Delta\psi_p$.

Additionally, we also test mitochondrial depolarization with KCl from purified nerve terminals loaded with $TMRM^+$, in order to have the control of our experience and confirming that both probes have distinctive behaviors. It is worth noting that oligomycin/FCCP and KCl have different degrees of mitochondrial depolarization which was also reported previously (Ward *et al.* 2000).

In this work, we brought new information about the particular vulnerability of the glutamatergic nerve terminals in early AD, where presynaptic mitochondria appear vulnerable. However, elucidate additionally mitochondrial parameters will able us to confront the results in order to identify what is compromising mitochondrial function.

6.CONCLUSION

In the present work, first we proposed to develop appropriate techniques to properly assess the bioenergetic status in *in situ* mitochondria. By measuring mitochondrial membrane potential, a central parameter of mitochondrial function, we could assess the mitochondrial status in an Aβ-based model of early AD. We report a reduction of mitochondrial membrane potential without any modification of the plasma membrane potential.

The present study reveals particular susceptibility of presynaptic mitochondria within glutamatergic nerve terminals in the hippocampus whereas no significant changes were observed in non-glutamatergic nerve terminals.

These results are in agreement with the contention that synaptic mitochondria are an important trigger of "synaptic apoptosis", contributing to synaptic dysfunction and degeneration in AD and further indicate glutamatergic terminals as primary targets of Aβ1-42-induced toxicity. This prompts the correction of synaptic mitochondria dysfunction as an increasingly and justifiable candidate to therapeutically alleviate early AD.

7. FUTURE PERSPECTIVES

Although this work has clarified some question regarding the role of synaptic mitochondria in an *in vitro* Aβ-based model of early AD, it has also raised several questions, to move forward.

First of all, it would be interesting to perform the same type of experiments *in vivo* using different animal models, namely, animals subjected to intracerebroventricular administration of $A\beta_{1-42}$ peptide and/or transgenic animal model of AD.

Additionally, since mitochondrial membrane potential and the role of mitochondria on Ca^{2+} handling are highly related, simultaneous monitoring mitochondria membrane potential and Ca^{2+} deregulation could elucidate if defects observed in mitochondrial membrane potential observed on synaptic mitochondria were cause or consequence of Ca^{2+} deregulation. This particular question could open another window, since if we verify that mitochondrial membrane potential defects is proceeded by Ca^{2+} deregulation, as previous shown in neurons (Nicholls 2006), we could perform pharmacology regarding presynaptic receptors.

Finally, clarify if and how, mitochondrial density vary within different types of nerve terminals it will be important to understand how synaptic mitochondria is regulated in active synapses.

8.REFERENCES

Alikhani, N. et al., 2011. Decreased proteolytic activity of the mitochondrial amyloid-β degrading enzyme, PreP peptidasome, in Alzheimer's disease brain mitochondria. *Journal of Alzheimer's Disease*, 27(1), pp.75–87.

Alonso-Nanclares, L. et al., 2008. Gender differences in human cortical synaptic density. *Proceedings of the National Academy of Sciences of the United States of America*, 105(38), pp.14615–9.

Anandatheerthavarada, H.K. et al., 2003. Mitochondrial targeting and a novel transmembrane arrest of Alzheimer's amyloid precursor protein impairs mitochondrial function in neuronal cells. *The Journal of Cell Biology*, 161(1), pp.41–54.

Aon, M.A. et al., 2012. Glutathione/thioredoxin systems modulate mitochondrial H2O2 emission: an experimental-computational study. *The Journal of General Physiology*, 139(6), pp.479–91.

Attwell, D. & Laughlin, S.B., 2001. An energy budget for signaling in the grey matter of the brain. *Journal of Cerebral Blood Flow and Metabolism*, 21(10), pp.1133–45.

Balaban, R.S., Nemoto, S. & Finkel, T., 2005. Mitochondria, oxidants, and aging. *Cell*, 120(4), pp.483–95.

Banaclocha, M.M. et al., 1997. N -Acetylcysteine protects against age-related increase in oxidized proteins in mouse synaptic mitochondria. *Brain Research*, 762, pp.256–258.

Bauer, M.F. & Neupert, W., 2001. Import of proteins into mitochondria: a novel pathomechanism for progressive neurodegeneration. *Journal of Inherited Metabolic Disease*, 24(2), pp.166–80.

Baxter, D.F. et al., 2002. A Novel Membrane Potential-Sensitive Fluorescent Dye Improves Cell-Based Assays for Ion Channels. *Journal of Biomolecular Screening*, 7(1), pp.79–85.

Begley, J.G. et al., 1999. Altered calcium homeostasis and mitochondrial dysfunction in cortical synaptic compartments of presenilin-1 mutant mice. *Journal of Neurochemistry*, 72(3), pp.1030–9.

Bell, K.F.S. et al., 2003. Structural involvement of the glutamatergic presynaptic boutons in a transgenic mouse model expressing early onset amyloid pathology. *Neuroscience Letters*, 353(2), pp.143–147.

Bell, K.F.S. & Cuello, A.C., 2006. Altered synaptic function in Alzheimer's disease. *European Journal of Pharmacology*, 545, pp.11–21.

Billings, L.M. et al., 2005. Intraneuronal Abeta causes the onset of early Alzheimer's disease-related cognitive deficits in transgenic mice. *Neuron*, 45(5), pp.675–88.

Billups, B. & Forsythe, I.D., 2002. Presynaptic mitochondrial calcium sequestration influences transmission at mammalian central synapses. *The Journal of Neuroscience*, 22(14), pp.5840–7.

Bobba, a et al., 2013. Mitochondrial respiratory chain Complexes I and IV are impaired by β-amyloid via direct interaction and through Complex I-dependent ROS production, respectively. *Mitochondrion*, 13(4), pp.298–311.

Boyd-Kimball, D. et al., 2005. Proteomic identification of proteins oxidized by Abeta(1-42) in synaptosomes: implications for Alzheimer's disease. *Brain Research*, 1044(2), pp.206–15.

Brown, M.R., Sullivan, P.G. & Geddes, J.W., 2006. Synaptic mitochondria are more susceptible to Ca2+ overload than nonsynaptic mitochondria. *The Journal of Biological Chemistry*, 281(17), pp.11658–68.

Buckner, R.L. et al., 2005. Molecular, structural, and functional characterization of Alzheimer's disease: evidence for a relationship between default activity, amyloid, and memory. *The Journal of Neuroscience*, 25(34), pp.7709–17.

Campanella, M. et al., 2009. IF(1): setting the pace of the F(1)F(o)-ATP synthase. *Trends in Biochemical Sciences*, 34(7), pp.343–50.

Canas, P.M. et al., 2009. Adenosine A2A receptor blockade prevents synaptotoxicity and memory dysfunction caused by beta-amyloid peptides via p38 mitogen-activated protein kinase pathway. *The Journal of Neuroscience*, 29(47), pp.14741–51.

Canas, P.M. et al., 2014. Predominant loss of glutamatergic terminal markers in a β-amyloid peptide model of Alzheimer's disease. *Neuropharmacology*, pp.6–11.

Caspersen, C. et al., 2005. Mitochondrial Abeta: a potential focal point for neuronal metabolic dysfunction in Alzheimer's disease. *Federation of American Societies for Experimental Biology*, 19(14), pp.2040–1.

Chan, D.C., 2006. Mitochondria: dynamic organelles in disease, aging, and development. *Cell*, 125(7), pp.1241–52.

Chiesa, R. et al., 2005. Bax deletion prevents neuronal loss but not neurological symptoms in a transgenic model of inherited prion disease. *Proceedings of the National Academy of Sciences of the United States of America*, 102(1), pp.238–43.

Choi, D.W., 1992. Excitotoxic cell death. *Journal of Neurobiology*, 23(9), pp.1261–76.

Choi, S.W. et al., 2012. No consistent bioenergetic defects in presynaptic nerve terminals isolated from mouse models of Alzheimer's disease. *The Journal of Neuroscience*, 32(47), pp.16775–84.

Cipolat, S. et al., 2004. OPA1 requires mitofusin 1 to promote mitochondrial fusion. *Proceedings of the National Academy of Sciences of the United States of America*, 101(45), pp.15927–32.

Cirrito, J.R. et al., 2008. Endocytosis is required for synaptic activity-dependent release of amyloid-beta in vivo. *Neuron*, 58(1), pp.42–51.

Cirrito, J.R. et al., 2005. Synaptic activity regulates interstitial fluid amyloid-beta levels in vivo. *Neuron*, 48(6), pp.913–22.

Clayton, E.L. & Cousin, M. a, 2009. The molecular physiology of activity-dependent bulk endocytosis of synaptic vesicles. *Journal of Neurochemistry*, 111(4), pp.901–14.

Coleman, P., Federoff, H. & Kurlan, R., 2004. A focus on the synapse for neuroprotection in Alzheimer disease and other dementias. *Neurology*, 63(7), pp.1155–1162.

Connors, B.W. & Long, M. a, 2004. Electrical synapses in the mammalian brain. *Annual Review of Neuroscience*, 27, pp.393–418.

Crouch, P.J. et al., 2005. Copper-dependent inhibition of human cytochrome c oxidase by a dimeric conformer of amyloid-beta1-42. *The Journal of Neuroscience*, 25(3), pp.672–9.

Culmsee, C. & Mattson, M.P., 2005. P53 in Neuronal Apoptosis. *Biochemical and Biophysical Research Communications*, 331(3), pp.761–77.

Davey, G.P., Peuchen, S. & Clark, J.B., 1998. Energy Thresholds in Brain Mitochondria: Potential involvement in neurodegeneration. *Journal of Biological Chemistry*, 273(21), pp.12753–12757.

David, G. & Barrett, E.., 2003. Mitochondrial Ca2+ uptake prevents desynchronization of quantal release and minimizes depletion during repetitive stimulation of mouse motor nerve terminals. *The Journal of Physiology*, 548(2), pp.425–38.

Degroot, A. et al., 2006. CB1 Receptor Antagonism Increases Hippocampal Acetylcholine Release: Site and Mechanism of Action. *Molecular Pharmacology*, 70(4), pp.1236–1245.

Devi, L. et al., 2006. Accumulation of amyloid precursor protein in the mitochondrial import channels of human Alzheimer's disease brain is associated with mitochondrial dysfunction. *The Journal of Neuroscience*, 26(35), pp.9057–68.

Díaz-Hernández, M. et al., 2002. Co-localisation of functional nicotinic and ionotropic nucleotide receptors in isolated cholinergic synaptic terminals. *Neuropharmacology*, 42(1), pp.20–33.

Dong, Z. et al., 2006. Calcium in cell injury and death. *Annual Review of Pathology*, 1, pp.405–34.

Du, H. et al., 2010. Early deficits in synaptic mitochondria in an Alzheimer's disease mouse model. *Proceedings of the National Academy of Sciences of the United States of America*, 107(43), pp.18670–5.

Du, H., Guo, L. & Yan, S.S., 2012. Synaptic mitochondrial pathology in Alzheimer's disease. *Antioxidants and Redox Signaling*, 16(12), pp.1467–75.

Duchen, M.R., 2000. Mitochondria and calcium: from cell signalling to cell death. *Journal of Physiology*, 529.1, pp.57–68.

Duchen, M.R., 2004. Mitochondria in health and disease: perspectives on a new mitochondrial biology. *Molecular Aspects of Medicine*, 25(4), pp.365–451.

Dunkley, P.R. et al., 1986. A rapid method for isolation of synaptosomes on Percoll gradients. *Brain Research*, 372(1), pp.115–129.

Dunkley, P.R., Jarvie, P.E. & Robinson, P.J., 2008. A rapid Percoll gradient procedure for preparation of synaptosomes. *Nature Protocols*, 3(11), pp.1718–28.

Echeverria, V. et al., 2004. Altered mitogen-activated protein kinase signaling, tau hyperphosphorylation and mild spatial learning dysfunction in transgenic rats expressing the beta-amyloid peptide intracellularly in hippocampal and cortical neurons. *Neuroscience*, 129(3), pp.583–92.

Ehrenberg, B. et al., 1988. Membrane potential can be determined in individual cells from the nernstian distribution of cationic dyes. *Biophysical Journal*, 53(5), pp.785–94.

Falkevall, A. et al., 2006. Degradation of the amyloid beta-protein by the novel mitochondrial peptidasome, PreP. *The Journal of Biological Chemistry*, 281(39), pp.29096–104.

Farkas, D.L. et al., 1989. Simultaneous imaging of cell and mitochondrial membrane potentials. *Biophysical Journal*, 56(6), pp.1053–69.

Frederick, R.L. & Shaw, J.M., 2007. Moving mitochondria: establishing distribution of an essential organelle. *Traffic*, 8(12), pp.1668–75.

Fremeau, R.T. et al., 2001. The Expression of Vesicular Glutamate Transporters Defines Two Classes of Excitatory Synapse. *Neuron*, 31, pp.247–260.

Fremeau, R.T. et al., 2002. The identification of vesicular glutamate transporter 3 suggests novel modes of signaling by glutamate. *Proceedings of the National Academy of Sciences of the United States of America*, 99(22), pp.14488–93.

Fujiyama, F., Furuta, T. & Kaneko, T., 2001. Immunocytochemical Localization of Candidates for Vesicular Glutamate Transporters in the Rat Cerebral Cortex. *The Journal of Comparative Neurology*, 435, pp.379–387.

Garcia, J. et al., 2010. Regulation of mitochondrial glutathione redox status and protein glutathionylation by respiratory substrates. *The Journal of Biological Chemistry*, 285(51), pp.39646–54.

Gillardon, F. et al., 2007. Proteomic and functional alterations in brain mitochondria from Tg2576 mice occur before amyloid plaque deposition. *Proteomics*, 7(4), pp.605–16.

Gillingwater, T.H. & Wishart, T.M., 2013. Mechanisms underlying synaptic vulnerability and degeneration in neurodegenerative disease. *Neuropathology and Applied Neurobiology*, 39, pp.320–334.

Gilman, C.P. & Mattson, M.P., 2002. Do apoptotic mechanisms regulate synaptic plasticity and growth-cone motility? *Neuromolecular Medicine*, 2(2), pp.197–214.

Gincel, D., Zaid, H. & Shoshan-Barmatz, V., 2001. Calcium binding and translocation by the voltage-dependent anion channel: a possible regulatory mechanism in mitochondrial function. *Biochemical Journal*, 358, pp.147–155.

Gleichmann, M. & Mattson, M.P., 2011. Neuronal calcium homeostasis and dysregulation. *Antioxidants and Redox Signaling*, 14(7), pp.1261–73.

Goedert, M. & Spillantini, M.G., 2006. A century of Alzheimer's disease. *Science*, 314(5800), pp.777–81.

Gras, C. et al., 2002. A third vesicular glutamate transporter expressed by cholinergic and serotoninergic neurons. *The Journal of Neuroscience*, 22(13), pp.5442–51.

Gray, E.G., 1959. Axo-somatic and axo-dendritic synapses of the cerebral cortex: an electron microscope study. *Journal of Anatomy*, 93, pp.420–33.

Guo, X. et al., 2005. The GTPase dMiro is required for axonal transport of mitochondria to Drosophila synapses. *Neuron*, 47(3), pp.379–93.

Guo, Z. et al., 2000. Beneficial effects of dietary restriction on cerebral cortical synaptic terminals: preservation of glucose and glutamate transport and mitochondrial function after exposure to amyloid beta-peptide, iron, and 3-nitropropionic acid. *Journal of Neurochemistry*, 75(1), pp.314–20.

Haass, C. & Selkoe, D.J., 2007. Soluble protein oligomers in neurodegeneration: lessons from the Alzheimer's amyloid beta-peptide. *Nature Reviews. Molecular Cell Biology*, 8(2), pp.101–12.

Haass, C. & Steiner, H., 2002. Alzheimer disease gamma-secretase: a complex story of GxGD-type presenilin proteases. *Trends in Cell Biology*, 12(12), pp.556–62.

Hagen, T.M. et al., 1997. Mitochondrial decay in hepatocytes from old rats: membrane potential declines, heterogeneity and oxidants increase. *Proceedings of the National Academy of Sciences of the United States of America*, 94(7), pp.3064–9.

Hansson, C. a et al., 2004. Nicastrin, presenilin, APH-1, and PEN-2 form active gamma-secretase complexes in mitochondria. *The Journal of Biological Chemistry*, 279(49), pp.51654–60.

Hansson Petersen, C. a et al., 2008. The amyloid beta-peptide is imported into mitochondria via the TOM import machinery and localized to mitochondrial cristae. *Proceedings of the National Academy of Sciences of the United States of America*, 105(35), pp.13145–50.

Hardy, J. & Selkoe, D.J., 2002. The amyloid hypothesis of Alzheimer's disease: progress and problems on the road to therapeutics. *Science*, 297(5580), pp.353–6.

Harris, K.M. & Weinberg, R.J., 2012. Ultrastructure of synapses in the mammalian brain. *Cold Spring Harbor Perspectives in Biology*, 4(5).

Hemachandra, R.P. & Flint, B.M., 2008. Amyloid beta, mitochondrial dysfunction and synaptic damage: implications for cognitive decline in aging and Alzheimer's disease. *Trends in Molecular Medicine*, 14(2), pp.45–53.

Herzog, E. et al., 2004. Localization of VGLUT3, the vesicular glutamate transporter type 3, in the rat brain. *Neuroscience*, 123(4), pp.983–1002.

Herzog, E. et al., 2001. The existence of a second vesicular glutamate transporter specifies subpopulations of glutamatergic neurons. *The Journal of Neuroscience*, 21(22), p.RC181.

Hisano, S. et al., 2002. Expression of inorganic phosphate/vesicular glutamate transporters (BNPI/VGLUT1 and DNPI/VGLUT2) in the cerebellum and precerebellar nuclei of the rat. *Brain Research Molecular Brain Research*, 107(1), pp.23–31.

Hollenbeck, P.J. & Saxton, W.M., 2005. The axonal transport of mitochondria. *Journal of Cell Science*, 118, pp.5411–9.

Hoppins, S., Lackner, L. & Nunnari, J., 2007. The machines that divide and fuse mitochondria. *Annual Review of Biochemistry*, 76, pp.751–80.

Hunsberger, J., Austin, D.R. & Henter, I.D., 2009. The neurotrophic and neuroprotective effects of psychotropic agents. *Dialogues in Clinical Neuroscience*, 11, pp.333–348.

Itoh, K. et al., 2013. Mitochondrial dynamics in neurodegeneration. *Trends in Cell Biology*, 23(2), pp.64–71.

Ivannikov, M. V, Sugimori, M. & Llinás, R.R., 2013. Synaptic vesicle exocytosis in hippocampal synaptosomes correlates directly with total mitochondrial volume. *Journal of Molecular Neuroscience*, 49(1), pp.223–30.

Johnson, L. V et al., 1981. Monitoring of relative mitochondrial membrane potential in living cells by fluorescence microscopy. *The Journal of Cell Biology*, 88(3), pp.526–35.

Jonas, E., 2006. BCL-xL regulates synaptic plasticity. *Molecular Interventions*, 6(4), pp.208–222.

Joyce, O.J.P. et al., 2003. Oxidative phosphorylation by in situ synaptosomal mitochondria from whole brain of young and old rats. *Journal of Neurochemistry*, 86(4), pp.1032–1041.

Kageyama, Y., Zhang, Z. & Sesaki, H., 2011. Mitochondrial division: molecular machinery and physiological functions. *Current Opinion in Cell Biology*, 23(4), pp.427–34.

Kamenetz, F. et al., 2003. APP Processing and Synaptic Function. *Neuron*, 37, pp.925–937.

Kaneko, T. & Fujiyama, F., 2002. Complementary distribution of vesicular glutamate transporters in the central nervous system. *Neuroscience Research*, 42(4), pp.243–50.

Kang, J. et al., 1987. The precursor of Alzheimer's disease amyloid A4 protein resembles a cell-surface receptor. *Nature*, 325, pp.733–736.

Kang, J.S. et al., 2008. Docking of axonal mitochondria by syntaphilin controls their mobility and affects short-term facilitation. *Cell*, 132(1), pp.137–148.

Kann, O. & Kova, R., 2007. Mitochondria and neuronal activity. *American Journal of Physiology. Cell Physiology*, 292, pp.C641–C657.

Kashani, A. et al., 2008. Loss of VGLUT1 and VGLUT2 in the prefrontal cortex is correlated with cognitive decline in Alzheimer disease. *Neurobiology of Aging*, 29(11), pp.1619–30.

Keelan, J., Vergun, O. & Duchen, M.R., 1999. Excitotoxic mitochondrial depolarisation requires both calcium and nitric oxide in rat hippocampal neurons. *The Journal of Physiology*, 520 Pt 3, pp.797–813.

Keller, J.N. et al., 2000. Amyloid beta-peptide effects on synaptosomes from apolipoprotein E-deficient mice. *Journal of Neurochemistry*, 74(4), pp.1579–86.

Keller, J.N. et al., 1997. Impairment of glucose and glutamate transport and induction of mitochondrial oxidative stress and dysfunction in synaptosomes by amyloid beta-peptide: role of the lipid peroxidation product 4-hydroxynonenal. *Journal of Neurochemistry*, 69(1), pp.273–84.

Kirvell, S.L., Esiri, M. & Francis, P.T., 2006. Down-regulation of vesicular glutamate transporters precedes cell loss and pathology in Alzheimer's disease. *Journal of Neurochemistry*, 98(3), pp.939–50.

Knobloch, M. et al., 2007. Intracellular Abeta and cognitive deficits precede beta-amyloid deposition in transgenic arcAbeta mice. *Neurobiology of Aging*, 28(9), pp.1297–306.

Köfalvi, A. et al., 2005. Involvement of cannabinoid receptors in the regulation of neurotransmitter release in the rodent striatum: a combined immunochemical and pharmacological analysis. *The Journal of Neuroscience*, 25(11), pp.2874–84.

Koike, T. et al., 2008. Axon & dendrite degeneration: its mechanisms and protective experimental paradigms. *Neurochemistry International*, 52(4-5), pp.751–60.

Kroemer, G., Galluzzi, L. & Brenner, C., 2007. Mitochondrial Membrane Permeabilization in Cell Death. *Physiological Reviews*, 87, pp.99–163.

Lai, J.C. & Clark, J.B., 1989. Isolation and Characterization of Synaptic and Nonsynaptic Mitochondria from Mammalian Brain. In *Carbohydrates and Energy Metabolism*. Clifton, NJ: Humana Press, pp. 43–98.

Lai, J.C.K. et al., 1977. Synaptic and non-synaptic mitochondria from rat brain: isolation and characterization. *Journul of Neurochemistry*, 28, pp.625–631.

Landis, D.M. et al., 1988. The organization of cytoplasm at the presynaptic active zone of a central nervous system synapse. *Neuron*, 1(3), pp.201–9.

Lee, C.W. & Peng, H.B., 2008. The Function of Mitochondria in Presynaptic Development at the Neuromuscular Junction. *Molecular Biology of the Cell*, 19, pp.150–158.

Lemasters, J.J. & Ramshesh, V.K., 2007. Imaging of mitochondrial polarization and depolarization with cationic fluorophores. *Methods in Cell Biology*, 80(06), pp.283–95.

Lewis, M. & Lewis, W., 1914. Mitochondria in Tissue Culture. *American Association for the Advancement of Science Stable*, 39(1000), pp.330–333.

Li, Z. et al., 2004. The importance of dendritic mitochondria in the morphogenesis and plasticity of spines and synapses. *Cell*, 119(6), pp.873–87.

Ligon, L. a & Steward, O., 2000a. Movement of mitochondria in the axons and dendrites of cultured hippocampal neurons. *The Journal of Comparative Neurology*, 427(3), pp.340–50.

Ligon, L. a & Steward, O., 2000b. Role of microtubules and actin filaments in the movement of mitochondria in the axons and dendrites of cultured hippocampal neurons. *The Journal of Comparative Neurology*, 427(3), pp.351–61.

Liguz-Lecznar, M. & Skangiel-Kramska, J., 2007. Vesicular glutamate transporters (VGLUTs): the three musketeers of glutamatergic system. *Acta Neurobiologiae Experimentalis*, 67(3), pp.207–18.

Lombe, A., Frachon, P. & Rojo, M., 2002. Mitochondrial Fusion in Human Cells Is Efficient , Requires the Inner Membrane Potential , and Is Mediated by Mitofusins. *Molecular Biology of the Cell*, 13, pp.4343–4354.

Lores-Arnaiz, S. & Bustamante, J., 2011. Age-related alterations in mitochondrial physiological parameters and nitric oxide production in synaptic and non-synaptic brain cortex mitochondria. *Neuroscience*, 188, pp.117–24.

Ma, H. et al., 2009. KIF5B motor adaptor syntabulin maintains synaptic transmission in sympathetic neurons. *The Journal of Neuroscience*, 29(41), pp.13019–29.

MacAskill, A.F., Atkin, T. a & Kittler, J.T., 2010. Mitochondrial trafficking and the provision of energy and calcium buffering at excitatory synapses. *The European Journal of Neuroscience*, 32(2), pp.231–40.

Macaskill, A.F. & Kittler, J.T., 2009. Control of mitochondrial transport and localization in neurons. *Trends in Cell Biology*, 20(2), pp.102–112.

Manji, H. et al., 2012. Impaired mitochondrial function in psychiatric disorders. *Nature Reviews. Neuroscience*, 13(5), pp.293–307.

Marcello, E. et al., 2012. Synaptic Dysfunction in Alzheimer's Disease M. R. Kreutz & C. Sala, eds. *Advances in Experimental Medicine and Biology*, 970, pp.573–601.

Martinez, M. et al., 1996. Age-related increase in oxidized proteins in mouse synaptic mitochondria. *Brain Research*, 731(1-2), pp.246–8.

Masliah, E. et al., 1989. Immunohistochemical quantification of the synapse-related protein synaptophysin in Alzheimer disease. *Neuroscience Letters*, 103(2), pp.234–9.

Massaad, C. a & Klann, E., 2011. Reactive oxygen species in the regulation of synaptic plasticity and memory. *Antioxidants and Redox Signaling*, 14(10), pp.2013–54.

Mattson, Keller, J. & Begley, J., 1998a. Evidence for synaptic apoptosis. *Experimental Neurology*, 153(1), pp.35–48.

Mattson, M., Partin, J. & Begley, J., 1998b. Amyloid beta-peptide induces apoptosis-related events in synapses and dendrites. *Brain Research*, 807(1-2), pp.167–76.

Mattson, M.P., Gleichmann, M. & Cheng, A., 2008. Mitochondria in neuroplasticity and neurological disorders. *Neuron*, 60(5), pp.748–66.

Mattson, M.P. & Kroemer, G., 2003. Mitochondria in cell death: novel targets for neuroprotection and cardioprotection. *Trends in Molecular Medicine*, 9(5), pp.196–205.

McInnes, J., 2013. Insights on altered mitochondrial function and dynamics in the pathogenesis of neurodegeneration. *Translational Neurodegeneration*, 2(1), p.12.

Medeiros, D.M., 2008. Assessing mitochondria biogenesis. *Methods*, 46(4), pp.288–94.

Mironov, S.L., 2007. ADP regulates movements of mitochondria in neurons. *Biophysical Journal*, 92(8), pp.2944–52.

Mokranjac, D. & Neupert, W., 2008. Energetics of protein translocation into mitochondria. *Biochimica et Biophysica Acta*, 1777(7-8), pp.758–62.

Moreira, P.I. et al., 2010. Mitochondrial dysfunction is a trigger of Alzheimer's disease pathophysiology. *Biochimica et Biophysica Acta*, 1802(1), pp.2–10.

Moreira, P.I. et al., 2006. The key role of mitochondria in Alzheimer's disease. *Journal of Alzheimer's Disease*, 9(2), pp.101–10.

Morris, R.L. & Hollenbeck, P.J., 1993. The regulation of bidirectional mitochondrial transport is coordinated with axonal outgrowth. *Journal of Cell Science*, 104, pp.917–27.

Mungarro-menchaca, X. et al., 2002. Beta-amyloid Peptide Induces Ultrastructural Changes in Synaptosomes and Potentiates Mitochondrial Dysfunction in the Presence of Ryanodine. *Journal of Neuroscience Research*, 68, pp.89–96.

Murphy, M.P., 2009. How mitochondria produce reactive oxygen species. *The Biochemical Journal*, 417(1), pp.1–13.

Naga, K.K., Sullivan, P.G. & Geddes, J.W., 2007. High cyclophilin D content of synaptic mitochondria results in increased vulnerability to permeability transition. *The Journal of Neuroscience*, 27(28), pp.7469–75.

Neupert, W. & Herrmann, J.M., 2007. Translocation of proteins into mitochondria. *Annual Review of Biochemistry*, 76, pp.723–49.

Nicholls, D.G., 2006. Simultaneous monitoring of ionophore- and inhibitor-mediated plasma and mitochondrial membrane potential changes in cultured neurons. *The Journal of Biological Chemistry*, 281(21), pp.14864–74.

Nicholls, D.G. & Budd, S.L., 2000. Mitochondria and neuronal survival. *Physiological Reviews*, 80(1), pp.315–60.

Nicholls, D.G. & Chalmers, S., 2004. The integration of mitochondrial calcium transport and storage. *Journal of Bioenergetics and Biomembranes*, 36(4), pp.277–81.

Nicholls, D.G. & Ward, M.W., 2000. Mitochondrial membrane potential and neuronal glutamate excitotoxicity: mortality and millivolts. *Trends in Neurosciences*, 23(4), pp.166–74.

Nickel, A., Kohlhaas, M. & Maack, C., 2014. Mitochondrial reactive oxygen species production and elimination. *Journal of Molecular and Cellular Cardiology*.

O'Connor, D.H., Wittenberg, G.M. & Wang, S.S.-H., 2005. Graded bidirectional synaptic plasticity is composed of switch-like unitary events. *Proceedings of the National Academy of Sciences of the United States of America*, 102(27), pp.9679–84.

Olichon, A. et al., 2003. Loss of OPA1 perturbates the mitochondrial inner membrane structure and integrity, leading to cytochrome c release and apoptosis. *The Journal of Biological Chemistry*, 278(10), pp.7743–6.

Oliveira, J.M.A., 2012. Mitochondrial Dysfunction in Neurodegenerative Disorders A. K. Reeve et al., eds. *Springer-Verlag London Limited*, pp.127–139.

Otera, H. et al., 2010. Mff is an essential factor for mitochondrial recruitment of Drp1 during mitochondrial fission in mammalian cells. *The Journal of Cell Biology*, 191(6), pp.1141–58.

Palmer, C.S. et al., 2011. MiD49 and MiD51, new components of the mitochondrial fission machinery. *EMBO reports*, 12(6), pp.565–73.

Patergnani, S. et al., 2011. Calcium signaling around Mitochondria Associated Membranes (MAMs). *Cell Communication and Signaling*, 9(1), p.19.

Perry, S.W. et al., 2011. Mitochondrial membrane potential probes and the proton gradient: a practical usage guide. *BioTechniques*, 50(2), pp.98–115.

Picconi, B., Piccoli, G. & Calabresi, P., 2012. Synaptic Dysfunction in Parkinson's Disease M. R. Kreutz & C. Sala, eds. *Advances in Experimental Medicine and Biology*, 970, pp.553–572.

Poon, H.F. et al., 2004. Free radicals: key to brain aging and heme oxygenase as a cellular response to oxidative stress. *The Journals of Gerontology. Series A, Biological Sciences and Medical Sciences*, 59(5), pp.478–93.

Rebola, N. et al., 2005. Adenosine A1 and A2A receptors are co-expressed in pyramidal neurons and co-localized in glutamatergic nerve terminals of the rat hippocampus. *Neuroscience*, 133(1), pp.79–83.

Reddy, P.H., 2011. Abnormal tau, mitochondrial dysfunction, impaired axonal transport of mitochondria, and synaptic deprivation in Alzheimer's disease. *Brain Research*, 1415, pp.136–48.

Reddy, P.H. & Beal, M.F., 2008. Amyloid beta, mitochondrial dysfunction and synaptic damage: implications for cognitive decline in aging and Alzheimer's disease. *Trends in Molecular Medicine*, 14(2), pp.45–53.

Richardson, J.. et al., 2003. Ultrastructural and behavioural changes precede amyloid deposition in a transgenic model of Alzheimer's disease. *Neuroscience*, 122(1), pp.213–228.

Rintoul, G.L. et al., 2003. Glutamate decreases mitochondrial size and movement in primary forebrain neurons. *The Journal of Neuroscience*, 23(21), pp.7881–8.

Rizzuto, R., 2001. Intracellular Ca2+ pools in neuronal signalling. *Current Opinion in Neurobiology*, 11, pp.306–311.

Rizzuto, R., Duchen, M.R. & Pozzan, T., 2004. Flirting in little space: the ER/mitochondria Ca2+ liaison. *Science's STKE: Signal Transduction Knowledge Environment*, 215, p.re1.

Rodrigues, D.I. et al., 2014. Synaptic and sub-synaptic localization of amyloid-β protein precursor in the rat hippocampus. *Journal of Alzheimer's Disease*, 40(4), pp.981–92.

Rottenberg, H. & Wu, S., 1998. Quantitative assay by flow cytometry of the mitochondrial membrane potential in intact cells. *Biochimica et Biophysica Acta*, 1404(3), pp.393–404.

Royle, S.J. & Lagnado, L., 2010. Clathrin-mediated endocytosis at the synaptic terminal: bridging the gap between physiology and molecules. *Traffic*, 11(12), pp.1489–1497.

Schäfer, M.K.-H. et al., 2002. Molecular cloning and functional identification of mouse vesicular glutamate transporter 3 and its expression in subsets of novel excitatory neurons. *The Journal of Biological Chemistry*, 277(52), pp.50734–48.

Scheff, S., DeKosky, S. & Price, D., 1990. Quantitative Assessment of Cortical Synaptic Density in Alzheimer's Disease. *Neurobiology of Aging*, 11(15), pp.29–37.

Scheff, S.W. et al., 2006. Hippocampal synaptic loss in early Alzheimer's disease and mild cognitive impairment. *Neurobiology of Aging*, 27(10), pp.1372–84.

Scott, I.D. & Nicholls, D.G., 1980. Energy transduction in intact synaptosomes. Influence of plasma-membrane depolarization on the respiration and membrane potential of internal mitochondria determined in situ. *Biochemical Journal*, 186(1), pp.21–33.

Selkoe, D.J., 2002. Alzheimer's disease is a synaptic failure. *Science*, 298(5594), pp.789–91.

Selkoe, D.J., 2001. Alzheimer's Disease: Genes, Proteins, and Therapy. *Physiological Reviews*, 81(2), pp.741–767.

Sheng, M., Sabatini, B.L. & Südhof, T.C., 2012. Synapses and Alzheimer's disease. *Cold Spring Harbor Perspectives in Biology*, 4(5).

Shepherd, G.M. & Harris, K.M., 1998. Three-dimensional structure and composition of CA3-->CA1 axons in rat hippocampal slices: implications for presynaptic connectivity and compartmentalization. *The Journal of Neuroscience*, 18(20), pp.8300–10.

Shoshan-Barmatz, V. & Ben-Hail, D., 2012. VDAC, a multi-functional mitochondrial protein as a pharmacological target. *Mitochondrion*, 12(1), pp.24–34.

Sirk, D. et al., 2007. Chronic exposure to sub-lethal beta-amyloid (Abeta) inhibits the import of nuclear-encoded proteins to mitochondria in differentiated PC12 cells. *Journal of Neurochemistry*, 103(5), pp.1989–2003.

Song, Z. et al., 2009. Mitofusins and OPA1 Mediate Sequential Steps in Mitochondrial Membrane Fusion. *Molecular Biology of the Cell*, 20, pp.3525–3532.

Starkov, A. a. & Fiskum, G., 2003. Regulation of brain mitochondrial H2O2 production by membrane potential and NAD(P)H redox state. *Journal of Neurochemistry*, 86(5), pp.1101–1107.

Stauch, K.L., Purnell, P.R. & Fox, H.S., 2014. Quantitative Proteomics of Synaptic and Nonsynaptic Mitochondria: Insights for Synaptic Mitochondrial Vulnerability. *Journal of Proteome Research*, 13, pp.2620–2636.

Strasser, A., Jost, P.J. & Nagata, S., 2009. The many roles of FAS receptor signaling in the immune system. *Immunity*, 30(2), pp.180–92.

Su, B. et al., 2010. Abnormal mitochondrial dynamics and neurodegenerative diseases. *Biochimica et Biophysica Acta*, 1802(1), pp.135–42.

Szabadkai, G. & Duchen, M.R., 2008. Mitochondria: the hub of cellular Ca2+ signaling. *Physiology*, 23, pp.84–94.

Sze, C.-I. et al., 2000. Selective regional loss of exocytotic presynaptic vesicle proteins in Alzheimer's disease brains. *Journal of the Neurological Sciences*, 175(2), pp.81–90.

Takahashi, R.H. et al., 2002. Intraneuronal Alzheimer Aβ42 Accumulates in Multivesicular Bodies and Is Associated with Synaptic Pathology. *The American Journal of Pathology*, 161(5), pp.1869–1879.

Takamori, S. et al., 2000. Identification of a vesicular glutamate transporter that defines a glutamatergic phenotype in neurons. *Nature*, 407, pp.189–194.

Takuma, K. et al., 2005. ABAD enhances Abeta-induced cell stress via mitochondrial dysfunction. *FASEB journal: official publication of the Federation of American Societies for Experimental Biology*, 19(6), pp.597–8.

Tampellini, D. et al., 2007. Internalized antibodies to the Abeta domain of APP reduce neuronal Abeta and protect against synaptic alterations. *The Journal of Biological Chemistry*, 282(26), pp.18895–906.

Tampellini, D. et al., 2009. Synaptic activity reduces intraneuronal Abeta, promotes APP transport to synapses, and protects against Abeta-related synaptic alterations. *The Journal of Neuroscience*, 29(31), pp.9704–13.

Tampellini, D. & Gouras, G.K., 2010. Synapses, synaptic activity and intraneuronal abeta in Alzheimer's disease. *Frontiers in Aging Neuroscience*, 2, pp.1–5.

Tang, Y. & Zucker, R.S., 1997. Mitochondrial involvement in post-tetanic potentiation of synaptic transmission. *Neuron*, 18(3), pp.483–91.

Terry, R.D. et al., 1991. Physical basis of cognitive alterations in Alzheimer's disease: synapse loss is the major correlate of cognitive impairment. *Annals of Neurology*, 30(4), pp.572–80.

Tretter, L., Chinopoulos, C. & Adam-Vizi, V., 1998. Plasma membrane depolarization and disturbed Na+ homeostasis induced by the protonophore carbonyl cyanide-p-trifluoromethoxyphenyl-hydrazon in isolated nerve terminals. *Molecular Pharmacology*, 53(4), pp.734–41.

Turrens, J.F., 2003. Mitochondrial formation of reactive oxygen species. *The Journal of Physiology*, 552, pp.335–44.

Twig, G., Elorza, AMolina, A., et al., 2008a. Fission and selective fusion govern mitochondrial segregation and elimination by autophagy. *The EMBO journal*, 27(2), pp.433–46.

Twig, G., Hyde, B. & Shirihai, O.S., 2008b. Mitochondrial fusion, fission and autophagy as a quality control axis: the bioenergetic view. *Biochimica et Biophysica Acta*, 1777(9), pp.1092–7.

Velliquette, R. a, O'Connor, T. & Vassar, R., 2005. Energy inhibition elevates beta-secretase levels and activity and is potentially amyloidogenic in APP transgenic mice: possible early events in Alzheimer's disease pathogenesis. *The Journal of Neuroscience*, 25(47), pp.10874–83.

Verstreken, P. et al., 2005. Synaptic mitochondria are critical for mobilization of reserve pool vesicles at Drosophila neuromuscular junctions. *Neuron*, 47(3), pp.365–78.

Ward, M.W. et al., 2000. Mitochondrial membrane potential and glutamate excitotoxicity in cultured cerebellar granule cells. *The Journal of Neuroscience*, 20(19), pp.7208–19.

Waters, J. & Smith, S.J., 2003. Mitochondria and release at hippocampal synapses. *Pflügers Archiv: European Journal of Physiology*, 447(3), pp.363–70.

Westermann, B., 2012. Bioenergetic role of mitochondrial fusion and fission. *Biochimica et Biophysica Acta*, 1817(10), pp.1833–8.

Whittaker, V.P., 1993. Thirty years of synaptosome research. *Journal of Neurocytology*, 22(9), pp.735–42.

Wojcik, S.M. et al., 2004. An essential role for vesicular glutamate transporter 1 (VGLUT1) in postnatal development and control of quantal size. *Proceedings of the National Academy of Sciences of the United States of America*, 101(18), pp.7158–63.

Wolfe, M.S. & Kopan, R., 2004. Intramembrane proteolysis: theme and variations. *Science*, 305(5687), pp.1119–23.

Wurtman, R.J., 1992. Choline metabolism as a basis for the selective vulnerability of cholinergic neurons. *Trends in Neurosciences*, 15(4), pp.117–22.

Yan, S. Du & Stern, D.M., 2005. Mitochondrial dysfunction and Alzheimer's disease: role of amyloid-beta peptide alcohol dehydrogenase (ABAD). *International Journal of Experimental Pathology*, 86(3), pp.161–71.

Yarana, C. et al., 2012. Synaptic and nonsynaptic mitochondria demonstrate a different degree of calcium-induced mitochondrial dysfunction. *Life Sciences*, 90(19-20), pp.808–14.

Yin, D. et al., 2012. Synaptic dysfunction in schizophrenia. M. R. Kreutz & C. Sala, eds. *Advances in Experimental Medicine and Biology*, 970, pp.493–516.

Ying, W., 2008. NAD+ and NADH in cellular functions and cell death: regulation and biological consequences. *Antioxidants and Redox Signaling*, 10(2), pp.179–206.

Youle, R.J. & Strasser, A., 2008. The BCL-2 protein family: opposing activities that mediate cell death. *Nature Reviews. Molecular Cell Biology*, 9(1), pp.47–59.

Zhang, Y. & Chan, D.C., 2007. New insights into mitochondrial fusion. *FEBS Letters*, 581(11), pp.2168–73.

Zhao, J. et al., 2011. Human MIEF1 recruits Drp1 to mitochondrial outer membranes and promotes mitochondrial fusion rather than fission. *The EMBO Journal*, 30(14), pp.2762–78.

Zhao, X.-L. et al., 2010. Expression of beta-amyloid induced age-dependent presynaptic and axonal changes in Drosophila. *The Journal of Neuroscience*, 30(4), pp.1512–22.

Zhu, X. et al., 2013. Abnormal mitochondrial dynamics in the pathogenesis of Alzheimer's disease. *Journal of Alzheimer's Disease*, 33 Suppl 1, pp.S253–62.

Zoratti, M. & Szabb, I., 1995. The mitochondrial permeability transition. *Biochimica et Biophysica Acta*, 1241, pp.139–176.

Zoratti, M. & Szabó, I., 1994. Electrophysiology of the inner mitochondrial membrane. *Journal of Bioenergetics and Biomembranes*, 26(5), pp.543–53.

Zorov, D.B., Juhaszova, M. & Sollott, S.J., 2006. Mitochondrial ROS-induced ROS release: an update and review. *Biochimica et Biophysica Acta*, 1757(5-6), pp.509–17.